WL-TR-97-3074

FLUTTER MODEL TECHNOLOGY

RON BUSAN
DYNAMIC ENGINEERING INC.
703 MIDDLE GROUND BOULEVARD
NEWPORT NEWS, VA 23606

January 1998

FINAL REPORT FOR 06/01/96-06/01/97

FLIGHT DYNAMICS DIRECTORATE
WRIGHT LABORATORY
AIR FORCE MATERIEL COMMAND
WRIGHT-PATTERSON AIR FORCE BASE OH 45433-7542

NOTICE

When Government drawings, specification, or other data are used for any purpose other than in connection with a definitely Government-related procurement, the United States Government incurs no responsibility or any obligation whatsoever. The fact that the Government may have formulated or in any way supplied the said drawings, specifications, or other data, is not to be regarded by implication, or otherwise in any manner construed, as licensing the holder, or any other person or corporation, or as conveying any rights or permission to manufacture, use, or sell any patented invention that may in any way be related thereto.

This report is releasable to the National Technical Information Service (NTIS). At NTIS, it will be available to the general public, including foreign nations.

This technical report has been reviewed and is approved for publication.

L J Huttsell

L. J. HUTTSELL
Project Engineer
Vibration & Aeroelasticity Branch

Michael L Zeigler

MICHAEL L. ZEIGLER
Core Area Leader
Structural Integrity of Aging Aircraft

T. M. Harris

T. M. HARRIS
Acting Chief, Vibration & Aeroelasticity Branch
Structures Division

If your address has changed, if you wish to be removed from our mailing list, or if the addressee is no longer employed by your organization, please notify, WL/FIBV, Bldg. 45, 2130 Eighth St Ste 1, WPAFB OH 45433-7542 to help us maintain a current mailing list.

Copies of this report should not be returned unless return is required by security consideration, contractual obligations, or notice on a specific document.

REPORT DOCUMENTATION PAGE

Form Approved
OMB No. 0704-0188

1. AGENCY USE ONLY (Leave Blank)	2. REPORT DATE	3. REPORT TYPE AND DATES COVERED
	JAN 1998	FINAL 06/01/96--06/01/97

4. TITLE AND SUBTITLE
FLUTTER MODEL TECHNOLOGY

5. FUNDING NUMBERS
C F33601-94-D-4016
PE 62201
PR 2401
TA LE
WU 00

6. AUTHOR(S)
Ron Busan

7. PERFORMING ORGANIZATION NAME(S) AND ADDRESS(ES)
DYNAMIC ENGINEERING, INC.
703 MIDDLE GROUND BOULEVARD
NEWPORT NEWS, VA 23606

8. PERFORMING ORGANIZATION REPORT NUMBER

9. SPONSORING / MONITORING AGENCY NAME(S) AND ADDRESS(ES)
FLIGHT DYNAMICS DIRECTORATE, WRIGHT LABORATORY
AIR FORCE MATERIAL COMMAND
WRIGHT PATTERSON AFB OH 45433-7542
POC: LARRY HUTTSELL, WL/FIBV (937) 255-7384

10. SPONSORING / MONITORING AGENCY REPORT NUMBER
WL-TR-97-3074

11. SUPPLEMENTARY NOTES

12a. DISTRIBUTION / AVAILABILITY STATEMENT
APPROVED FOR PUBLIC RELEASE; DISTRIBUTION IS UNLIMITED.

12b. DISTRIBUTION CODE

13. ABSTRACT *(Maximum 200 words)*

Wind tunnel testing of dynamically scaled models plays a key role in assuring that new or modified aircraft will be free of flutter within their flight envelopes. Dynamically scaled models are also widely used in research studies such as active control of aeroelastic response, buffet alleviation, and validation of theoretical or computational methods. This paper summarizes many of the critical design consideration involved with designing and fabricating flutter model hardware once the basic requirements have been determined. Topics discussed include: spar design, stress skin construction, hinged control surfaces, instrumentation, calibration, load testing, and a case study for supersonic F-22 flutter model components.

14. SUBJECT TERMS
Flutter, Flutter Model Design, Wind Tunnel Models, Composites

15. NUMBER OF PAGES
57

16. PRICE CODE

17. SECURITY CLASSIFICATION	18. SECURITY CLASSIFICATION OF THIS PAGE	19. SECURITY CLASSIFICATION OF ABSTRACT	20. LIMITATION OF ABSTRACT
UNCLASSIFIED	UNCLASSIFIED	UNCLASSIFIED	SAR

NSN 7540-01-280-5500

Standard Form 298 (Rev. 2-89)
Prescribed by ANSI Std. Z39-18
298-102

TABLE OF CONTENTS

Section	*Title*	*Page No.*
1.0	**INTRODUCTION**	**1**
2.0	**MODEL DESIGN BASICS**	**2**
	2.1 Model Scaling	2
	2.2 Model Configurations	3
	2.3 Model Mounting System	5
	2.4 Types of Construction	6
	2.5 Materials Used	9
3.0	**DESIGN DETAILS**	**14**
	3.1 Plate Construction	14
	3.2 Beam/Spar/Pod Construction	15
	3.3 Stress Skin Construction	24
	3.4 Replica Construction	25
	3.5 Hinged Control Surfaces	25
4.0	**INSTRUMENTATION**	**29**
	4.1 Strain Gage Bridges	29
	4.2 Accelerometers	29
	4.3 Dynamic Pressure Transducers and Piezoelectric Strain Elements	29
5.0	**MODEL CALIBRATION TECHNIQUES AND "TUNING"**	**30**
	5.1 Stiffness	30
	5.2 Mass and Inertia Properties	32
	5.3 Mounting Options	34
	5.4 Natural Frequency Determination	36
	5.5 Mode Shapes	37
	5.6 Stiffness Tuning of Spars and Flexures	39
	5.7 Mass Ballasting	39
	5.8 FEM Correlation	40
6.0	**LOAD TESTS TO VERIFY STRUCTURAL INTEGRITY**	**41**
	6.1 Point Loads	41
	6.2 Distributed Loads	42
7.0	**DOCUMENTATION**	**45**
	7.1 Calibration Report	45
	7.2 Stress Report	45
	7.3 Support System Stability Analysis	45

8.0 THE DESIGN AND ANALYSIS PROCESS - A CASE STUDY 46
8.1 Methodology for Converting Specifications 47
8.2 Material Selection and Property Verification 47
8.3 Stiffness and Strength Evaluation 48
8.4 Weight Evaluation and Control 49
8.5 Model Scale FEM 50
8.6 Model Stress Analysis 51
8.7 Vertical Stabilizer Construction Details 52

1.0 INTRODUCTION

Wind tunnel testing of dynamically scaled models plays a key role in assuring that new or modified aircraft will be free of flutter within their flight envelopes. Typically, about one-quarter of the total resources allocated to the flutter clearance of fighter type aircraft are for wind tunnel flutter model test programs. Dynamically scaled models are also widely used in research studies such as active control of aeroelastic response, buffet alleviation, and validation of theoretical or computational methods.

The purpose of this paper is to summarize the critical design considerations involved with designing and fabricating flutter model hardware once the basic requirements have been determined. An exhaustive treatment of all the analytical and testing considerations associated with flutter phenomena is beyond the scope of this work. Analytical and testing techniques will only be discussed with regard to their relation to the design, fabrication, and calibration of the hardware prior to tunnel testing.

The paper is organized as follows:

- Sections 2 and 3 present some design basics followed by a more detailed discussion of the design process for specific types of flutter model construction.
- Sections 4 through 7 discuss instrumentation, calibration techniques, load testing, and documentation.
- Section 8 is a case study of the design and analysis process for a set of supersonic flutter model components.

The design, analysis, fabrication, and calibration of flutter models involves many challenging and critical techniques. Engineers sometimes accuse the flutter model designer of practicing a mixture of intuition and art in addition to sound engineering practice. The intuition and art in many ways determine the eventual technical success of the model, but only if it is otherwise soundly engineered using techniques such as those presented in this paper.

2.0 MODEL DESIGN BASICS

2.1 Model Scaling

The selection of scale factors is a critical first step of any flutter model program. The first parameter to be selected is the model size, which determines the geometric scale factor, or the length ratio. It is usually desirable to make flutter models as large as possible for ease of fabrication and structural strength, as well as to make it easier to install instrumentation. Flutter models are typically larger relative to tunnel size than are conventional aerodynamic models. Although no absolute maximum ratio of model size to wind-tunnel size has been established, it is generally believed that it is desirable that the span of the model be less than 60 percent of the test section width for transonic tests where compressibility effects are important. Models for use at low speeds (compressibility effects not important) may have a larger span, perhaps as large as 75 percent of the test section width.

The fluid density is another parameter which is selected. Normally there will be one point in the full-scale operational envelope that will be simulated exactly during the wind-tunnel test. Testing will be conducted, of course, at other conditions, but the model will be slightly "out of scale." Generally, a density that is well up in the tunnel capability will be selected. The larger the test density for the model, the heavier the model can be made. Usually the heavier an aeroelastic model is, the easier it is to design and fabricate. Very lightweight structures are not only fragile, but are also costly to make and maintain.

For tests where compressibility effects are not important a wind-tunnel velocity will be selected to represent some full-scale velocity. These velocities can be the same or different in value. For tests where compressibility effects are important, there must be a match between model and full-scale Mach numbers so that the velocity scale factor becomes in effect a speed-of-sound scale factor.

There are essentially two classes of flutter models: low-speed models and high-speed models.

- For low speed models compressibility effects are not important so that the Mach number $(M=V/a)$ parameter is not matched between the model and the full-scale vehicle. The parameters that are always matched are the reduced frequency $(k=lw/V)$ and the mass ratio $(M=m/\rho V)$. It is also possible to match the Froude number $(F_N=V^2/lg)$, if that is desired. Froude number is an important parameter in instances where it is desirable to match static deflections of the vehicle due to gravity.
- For high speed models compressibility effects are important, and it is mandatory that the Mach numbers match. In addition, the reduced frequency and mass ratio will also be matched. It is not possible to satisfy Mach number, reduced frequency, and Froude number for a wind tunnel test with air as a test medium. It is possible, however, to match these parameters in another test medium, e.g., a nominal one-quarter size model tested in freon-12, which has a speed of sound (velocity) about one-half that of air, will satisfy these parameters. Due to environmental impact freon-12 is now being replaced with R134A at several test facilities.

2.2 Model Configurations

Most flutter models will fit into one of the following three configurations: component models, semispan models, or a model of the complete vehicle. For a particular aircraft program the models fabricated and tested will often progress through these configurations – initially starting with individual components, and ending with a model of the complete assembled vehicle.

Component Models

Component models are used to evaluate the dynamic characteristics of individual aircraft elements such as a wing, vertical tail, or horizontal. Since only an individual component is mounted in the tunnel, the scale factor can be larger, which often simplifies construction. Rudders and wing control surfaces will often be fabricated as separate elements, but are normally wind tunnel tested as part of a vertical tail or wing assembly. Component models are often mounted rigidly to a tunnel wall, although in some cases the attachment may incorporate springs or flexures to simulate a known mounting or actuator stiffness. ***Figure 2.2a*** shows a set of wing component flutter models.

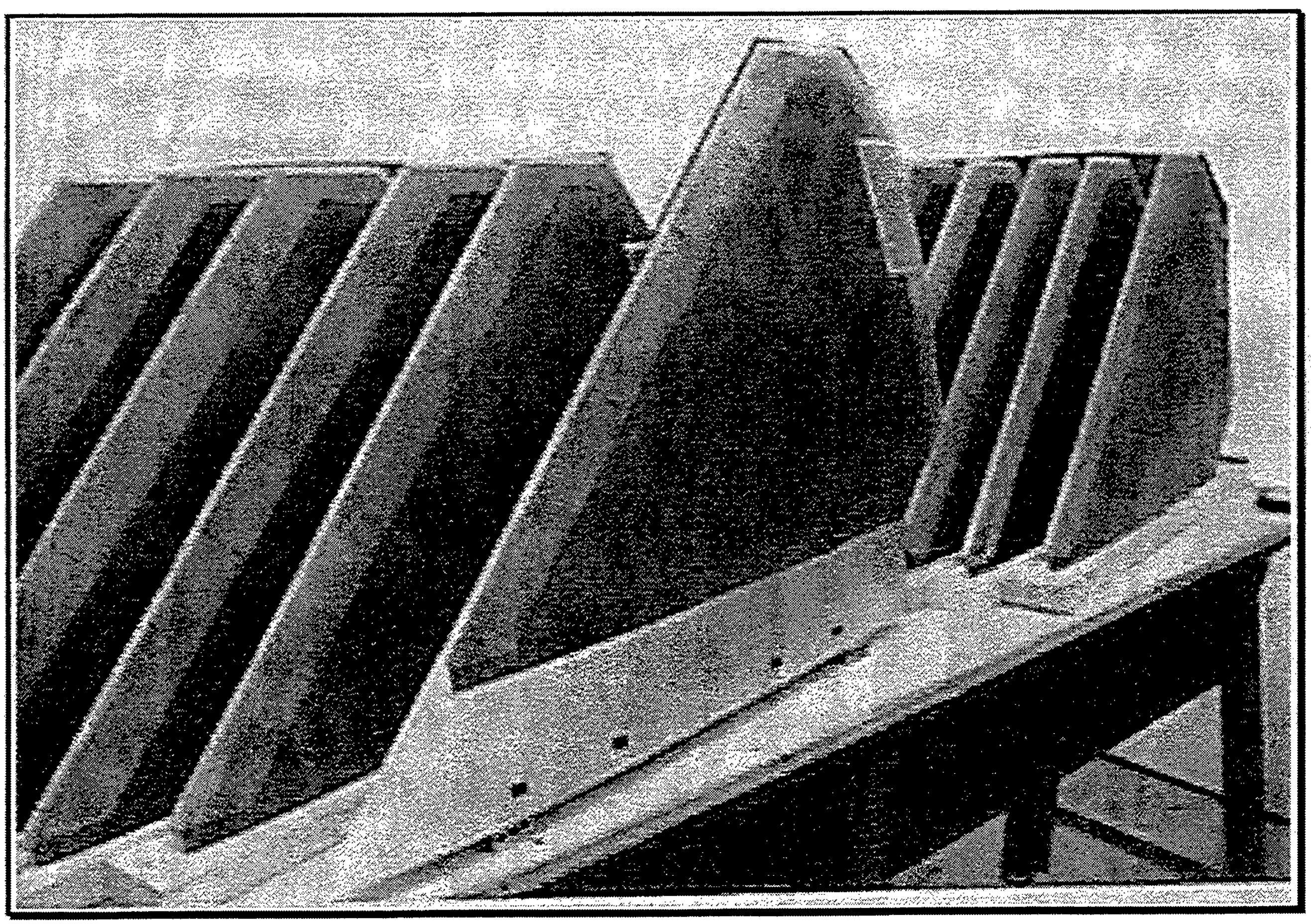

Figure 2.2a F-22 Supersonic Wing Flutter Models

Semispan Models

If the results of testing individual components and sub-assemblies yield satisfactory results, then a semispan model may be used to evaluate some of the interactions between components in the presence of a fuselage. Although a semispan model will not represent all the dynamic modes of the flight vehicle, it is considerably less expensive than a full model, and it will give significant information which cannot be obtained from individual component tests. ***Figure 2.2b*** is an example of a semispan model.

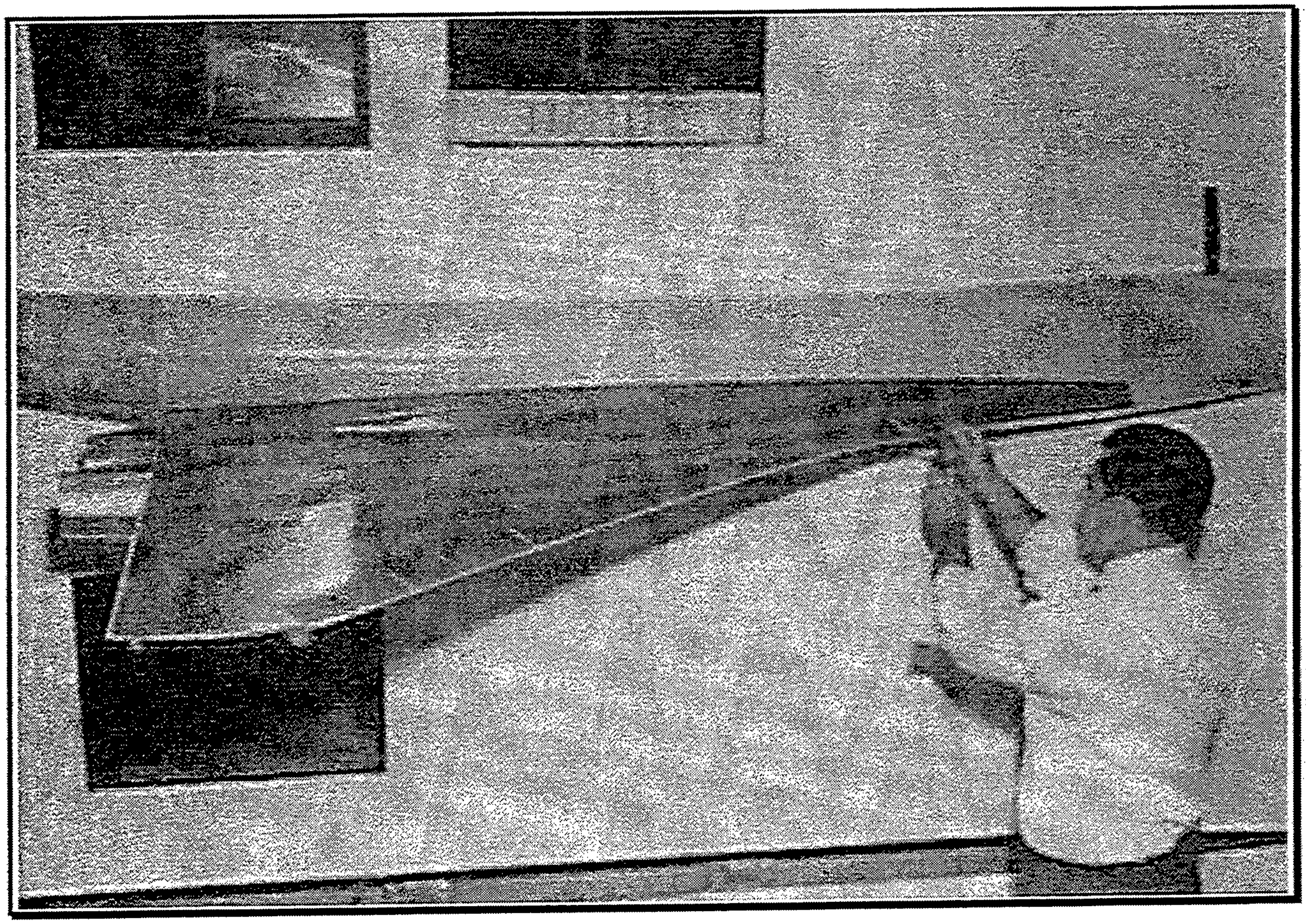

Figure 2.2b Boeing SST Semispan Transonic Flutter Model

Complete Vehicle

A flutter model of the entire assembled vehicle configuration will yield results giving the most complete information about the dynamic characteristics of the flight vehicle. However, because of the complexity of interactions between the various elements of the aircraft it may be difficult to interpret the results unless there has been previous testing of individual components. A flutter model of a complete aircraft assembly can also be relatively expensive, which is why models of simpler configurations will often be done to obtain preliminary data. ***Figure 2.3*** is an example of a flutter model of a complete flight vehicle.

2.3 Model Mounting Systems

The mounting system for a flutter model must support the model in its proper position in the tunnel while simultaneously allowing sufficient motion so that the modes for the model can be evaluated. Support systems which have been used include cantilever mounts for individual components, stings, struts, four bar linkages, vertical rod and gimbal, cables, and 2-wire flying cable systems. Cantilevered models are used when it is not necessary to simulate the rigid body modes. In most cases the designer will attempt to have the mounting system allow three symmetric and three antisymmetric rigid body degrees of freedom with frequencies at least 30% below the lowest predicted flutter frequency.

Each of the support mounting systems has particular advantages and disadvantages. Because this paper focuses on the flutter model components themselves, a detailed treatment of these support systems is beyond the scope of this report. Frequently the particular support mounting system used will be determined by the facility where testing will occur, and further information can be obtained from the facilities directly. The following figure shows an F-18 E/F flutter model mounted on a cable/wire support system in the Transonic Dynamics Tunnel (TDT) at NASA Langley.

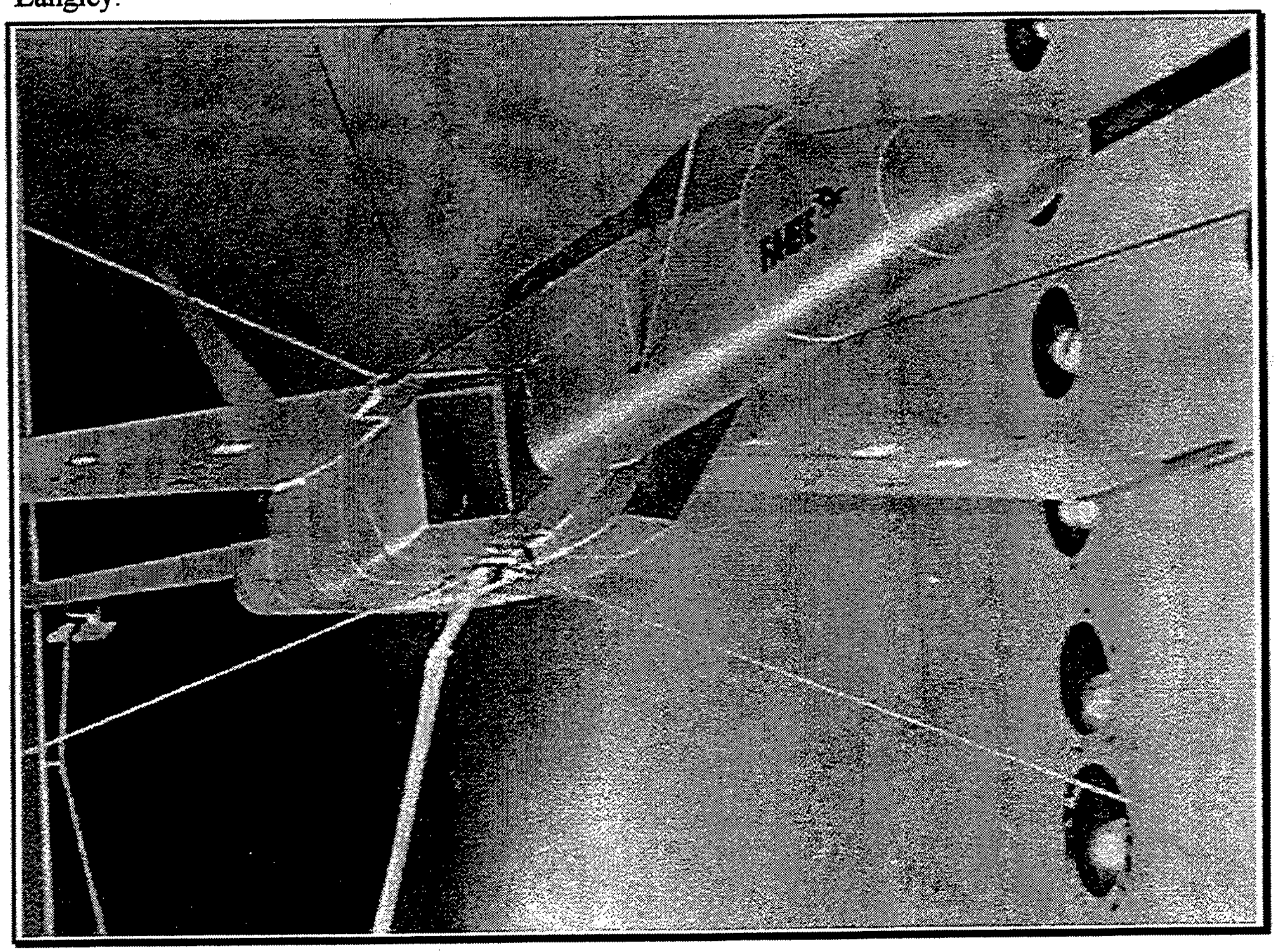

Figure 2.3 F-18 E/F Flutter Model

2.4 Types of Construction

The type of flutter model construction is usually determined by the specific test objectives (e.g. flutter trend studies, research, or flutter clearance of particular aircraft designs). The four basic types of construction are:

- plate
- beam/spar/pod
- stress skin
- replica

Simple trend studies or research can often be cost effectively evaluated using plate construction or a simplified beam/spar/pod model. Flutter clearance of aircraft designs will generally require more complicated beam/spar/pod models or stress skin/replica construction because of the need to accurately represent an actual aircraft structure.

The following paragraphs briefly describe each of these types of construction. A detailed discussion of the design parameters associated with each approach is contained in Section 3.0.

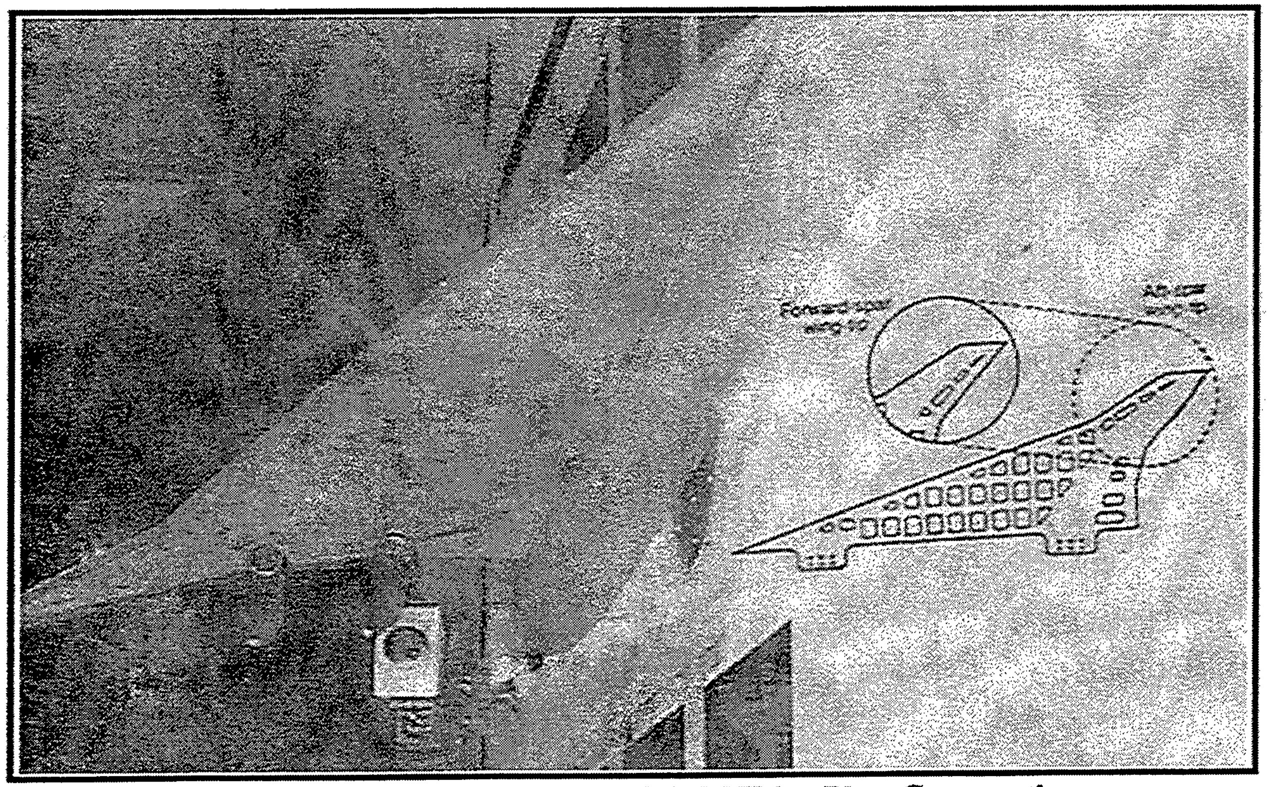

Figure 2.4a Arrow Wing Research Model Using Plate Construction

Plate Construction

One method for matching the stiffness distribution of low aspect-ratio lifting surfaces is to use some variation of a plate as the main structural element. This approach has the advantage of providing a broad surface to which shaped elements can be mounted to simulate the proper external aerodynamic contour.

Since a constant thickness plate will rarely provide the required stiffness distribution, some means must be provided for varying the stiffness distribution across the plate. This can be done by "building up" sections of the plate to increase stiffness, making "cutouts" in the plate to reduce stiffness, "contouring" the surface of the plate, or some combination of each.

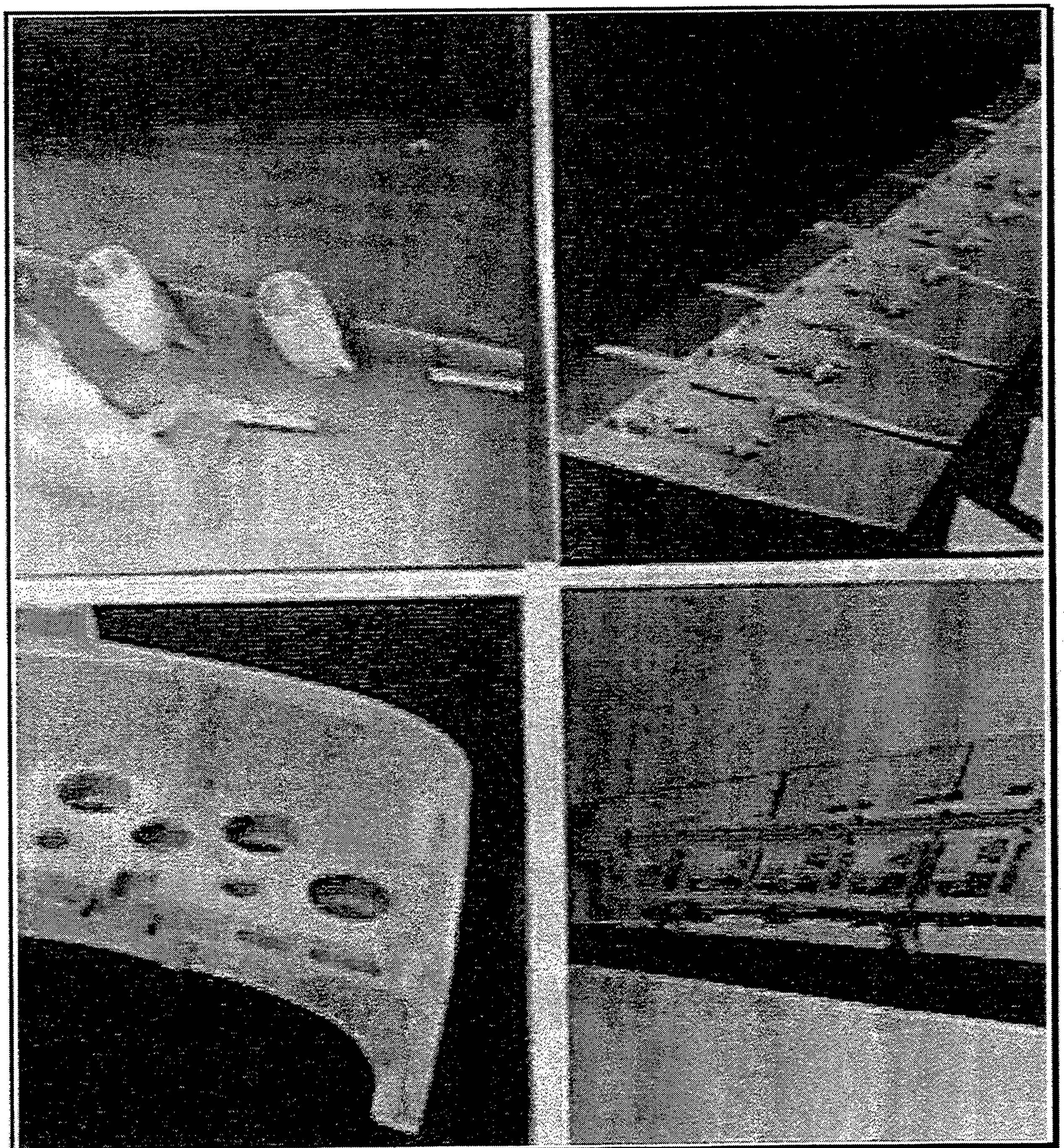

Figure 2.4b Views of a CX Flutter Model Using Spar/Beam/Pod Construction

Beam/Spar/Pod Construction

Figure 2.4b illustrates beam/spar/pod flutter model construction. In this method a spar or beam element simulates the entire stiffness of the component. External "pods" attached to the spar provide the proper external aerodynamic shape. These pods typically have small gaps between them, with each pod attached to the spar at only one location. This minimizes the influence of the pods on the stiffness distribution of the component. The pods are normally constructed of lightweight materials, although "ballast weights" may be added later to properly simulate the mass properties of the overall component.

Figure 2.4c Stress Skin Construction

Stress Skin Construction

For stress skin construction the skins forming the external contour carry a significant portion of the loads, and largely determine the dynamic characteristics of the model. Because the outer skin is intended to transmit loads, there are typically no "gaps" in the external shell. The core of a stress skin component will often be filled with a lightweight honeycomb or foam material. This type of construction is very common for high speed flutter models where the effects of "gaps" and discontinuities in the surface are much more critical to the flutter mechanisms.

Replica Construction

Replica construction involves duplicating the construction methodology for the full-scale design when making the model. Since almost all modern aircraft employ an integral skin/internal structure to transmit loads, this is typically a very difficult and costly construction method to use. Replica construction will almost always require extensive use of finite element modeling (FEM) because the interrelationship between skins and internal structure for the full-scale design is not always easy to assess. Except for very simple components replica construction often cannot be followed stringently because of unequal scaling factors, mounting constraints, and the particular requirements of the planned testing.

2.5 Materials Used

The following table includes some materials frequently used in flutter model construction. "E" is the modulus of elasticity, "G" is the modulus of rigidity, and "F_{tu}" is ultimate tensile strength.

Material	E (psi)	G (psi)	Density (lb/in^3) *Wt/Area (lb/in^2)*	F_{tu} (lb/in^2)
2024 Aluminum	10.5×10^6	4.0×10^6	.100	-----
Magnesium	6.5×10^6	2.4×10^6	.065	-----
Titanium	16.5×10^6	6.1×10^6	.163	-----
Steel	29.0×10^6	11.6×10^6	.280	-----
0-90° Fiberglass	3.5×10^6	$.40 \times 10^6$	.068	47,000
±45° Fiberglass	1.25×10^6	1.5×10^6	.068	20,000
0-90° Graphite	10.5×10^6	1.0×10^6	.057	90,000
±45° Graphite	3.8×10^6	4.0×10^6	.057	25,000
0-90° Kevlar	5.1×10^6	$.32 \times 10^6$	.048	75,000
±45° Kevlar	2.1×10^6	2.4×10^6	.048	30,000
Balsa (// to grain)	5000	200	.005	800
HRH 10-1/8 -1.8 Honeycomb	-----	-----	.00104	-----
HRH 10-1/8 - 3.0 Honeycomb	-----	-----	.00174	-----
1/64" Aircraft Plywood (3 ply)	-----	-----	*.0004586*	-----
1/32" Aircraft Plywood (3 ply)	-----	-----	*.000926*	-----
1/16" Aircraft Plywood (3 ply)	-----	-----	*.001565*	-----
1/8" Aircraft Plywood (5 ply)	-----	-----	*.002372*	-----
Tungsten	-----	-----	.67	-----

It should also be noted that the values in the table are averages. The values for metals do not vary much, but composite properties can deviate widely depending on the particular fibers used, the weave pattern, the layup process, etc. For example, the author is aware of a case where one graphite fabric was substituted for another. The brand of fibers, density, number of strands in each direction were all identical. The only thing that differed was the weave pattern, but this was enough to change the effective "E" value by 20%.

For composite layups it is a good practice to make up calibration samples using the same process planned for the spars. "E" and "G" values derived from such samples may vary significantly from those obtained from published data sheets. This is not to imply that manufacturers are not properly representing their products. Rather this is just a recognition of how "process dependent" the properties of composite layups can be. The flutter model designer must recognize and accommodate this reality of composite materials in flutter model applications.

There is also a common misconception that composites will always provide a stronger/stiffer structure for less overall weight. It is true that composites typically provide a better strength/stiffness to ***weight*** ratio when only one direction is important. However, in many cases spars or skins will experience loading in multiple directions, and it is necessary to design the structure with significant strength/stiffness along multiple axes. In these cases metal may prove to be more efficient not only because its material properties are isotropic, but also because the strength/stiffness to ***volume*** ratio is typically better for metals than for composites. This can be a significant factor for highly load structures where the external contour is fixed.

This author is aware of several instances involving relatively thin members when then strongest/stiffest sandwich structure was obtained from steel skins over a honeycomb core. This was because the steel skins were thinner and thus had a greater average distance from the neutral axis. (The composite skins needed to be thicker, and as the skin thickness increases inward from the external geometry the effectiveness of the additional material decreases.)

The three most common composite materials used for flutter model construction are graphite, fiberglass, and Kevlar. Each of these has its own particular advantages and disadvantages.

Graphite

Graphite materials generally provide a higher strength/stiffness to weight ratio than fiberglass. This is its primary advantage. The main disadvantage of graphite is its cost. Graphite also does not sand to quite as smooth a surface as fiberglass unless care it taken with regard to the resin content.

Graphite has an extremely low coefficient of thermal expansion. This can either be an advantage or a disadvantage depending on the requirements. If a graphite component is cured at elevated temperatures in an aluminum mold the resulting part will be larger because of the expansion of the mold. As the aluminum mold cools it will contract, but the graphite will not. This can cause difficulty in removing the part from the mold. For longer parts the dimensional changes may be significant enough that they will need to be accounted for during the design process.

Fiberglass

Fiberglass is readily available, relatively inexpensive, and easy to work with. This is usually the first choice of composite materials unless the model requirements dictate otherwise. The main disadvantage of fiberglass is that it is somewhat heavier and not as stiff or strong as an equivalent weight of graphite.

Kevlar

The main advantages of Kevlar is its toughness, abrasion resistance, and light weight. Graphite and fiberglass can be somewhat brittle, and individual fibers will fracture easily. Kevlar is much tougher, which is the reason it is frequently employed in bullet proof vests and lightweight armor for military applications. Generally the stiffness properties of Kevlar are less than graphite, but higher than fiberglass. Kevlar is also relatively expensive, and it is difficult to cut or sand because the individual fibers will resist shearing.

Kevlar is occasionally used in flutter models for applications where toughness is needed. Section 8.0 describes how it was used to solve a particular design challenge on a supersonic flutter model component.

Combinations of Composite Materials

It is possible to mix the various composite materials together in a single layup to make the best use of the favorable characteristics of each. For example, the outer layer of the skins on some of the supersonic flutter model components described in Section 8.0 was fiberglass fabric, and the remainder was graphite unidirectional tape. Whenever combinations of materials are put together it is advisable to make samples to ensure that there are no unforeseen difficulties. The initial skin layups just referred to curled up like potato chips because the fiberglass on the outer surface contracted significantly as the cured layup cooled, but the adjacent graphite did not. This made it necessary to use a vacuum "bag" to flatten out the skins and hold them tight against the core material while the adhesive bond was curing.

Fabrics, Unidirectional Tapes, and Roving

Woven fabrics are convenient to use for skin layups. Woven fabric also provides the most suitable external finish on a skin because interwoven fiber bundles are less likely to be pulled loose from a scratch or scrape. For this reason a thin layer of woven fabric is often placed as the most exterior layer of the skin, even when the main layup consists primarily of unidirectional tape. Woven fabric also tends to be more isotropic with regard to its material properties. This inherently makes a skin layup made from woven fabric less likely to warp or have interlaminar stress problems.

Unidirectional tapes have the advantage of providing the highest strength and stiffness associated with a single direction. In applications where it is essential to achieve a strength or stiffness in one direction which is significantly higher than for others, unidirectional tape may be the best alternative. Some of the disadvantages of unidirectional tape are:

- they are more subject to damage due to kinking of fibers or surface scrapes
- layups are more difficult to analyze with regard to stiffnesses and strengths in the off-axis directions
- they are normally only available pre-impregnated with resin
- warping of the skins is more likely due to the non-isotropic mature of the material
- they are much more sensitive to "fiber wash" (local changes in fiber orientation)

The previous table of material properties does not include any values for unidirectional composites. The reason for this is that unidirectional composites present greater challenges with regard to the stress analysis, and their properties are even more process dependent than fabrics. The very high published "E" values for unidirectional layups can only be achieved with careful control of the fabrication process. For example, the author is aware of a spar that was designed using an extensive amount of unidirectional graphite. The resulting spar stiffness was about 15% lower than expected due to small deviations in the mold pressure which caused the fibers to change their orientation slightly ("fiber wash"). Understanding and accounting for all the possible variables associated with a unidirectional composite layup can be a tedious process requiring multiple sample parts. While this may be warranted for mass production, it is usually not the most effective method to produce a flutter model component.

Roving consists of a continuous fiber bundle which can be used to create a composite structure using a filament winding machine. This approach is much more suited to mass production items for commercial industry. It is listed here only because it could be considered as an alternative fabrication method for certain simple spar configurations.

Dry versus Pre-Impregnated With Resin

Woven fabrics and roving are available as "dry" material consisting only of the fiber strands, or pre-impregnated with resin by the manufacturer. Unidirectional tape is normally only available pre-impregnated with resin. This is because the unidirectional fiber strands would simply fall apart if not "stuck" together with the resin. The following tables highlight the major advantages and disadvantages of using dry or pre-impregnated materials.

Dry:

Advantages	***Disadvantages***
easy storage, and no shelf life considerations	unidirectional tape not available
can be cured at room temperature - and therefore can be used with wooden molds or patterns, wood internal structure, and low temperature adhesives	resin content of final layup is a function of the particular fabrication procedure followed, thus making it more difficult to control

Pre-Impregnated With Resin:

Advantages	***Disadvantages***
resin content of final layup very predictable	must be stored in a freezer – has a limited shelf life
unidirectional tape available	usually must be cured at elevated temperatures – therefore usually must use composite or metal molds/patterns, and must consider temperature effects on wood and other materials subjected curing temperatures

3.0 DESIGN DETAILS

Sections 3.1 through 3.4 are descriptions of the design process for the four most common methods of flutter model construction. Section 3.5 deals with the specific subject of hinged control surfaces.

3.1 Plate Construction

Except for the most elementary of designs it is difficult to calculate a set of influence coefficients for a plate structure. Typically a finite element model (FEM) will be required to iterate to an acceptable design using plate construction.

Built-Up Plate Structure

A "built-up" plate structure is typically fabricated by bonding together constant thickness sheets of material as shown in **Figure 3.1a**. Aluminum and magnesium are the most common metal materials used in plate construction. For built-up plate construction composite materials can provide the design flexibility for adding plys to "tune" a plate structure up to match a particular stiffness distribution once the initial plate fabrication is complete. "Tuning" of flutter model structural elements is discussed in Section 5.6.

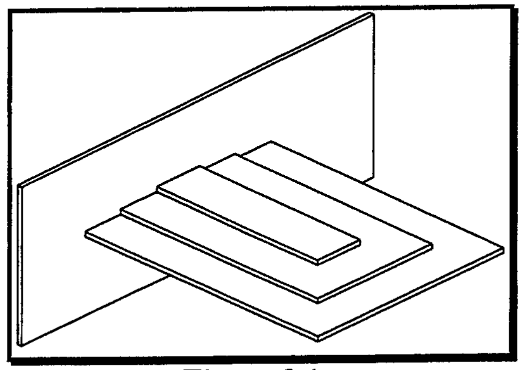

Figure 3.1a
Build-up Plate Structure

Constant-Thickness Plate With Cutouts

A second approach is to start with a constant thickness plate which matches the "stiffest" portions of the target distribution. Other areas of the plate are then "cut out" to reduce the stiffness in the discrete areas corresponding to lower stiffnesses on the target distribution. **Figure 3.1b** shows a constant-thickness plate with circular cutouts. The shape, size, and number of plate cutouts is determined based on fabrication considerations, and on what particular configuration which the finite element model indicates will best match the targets. If larger and larger rectangular holes are used, the remaining plate structure will approach a beam network like that discussed in Section 3.2.

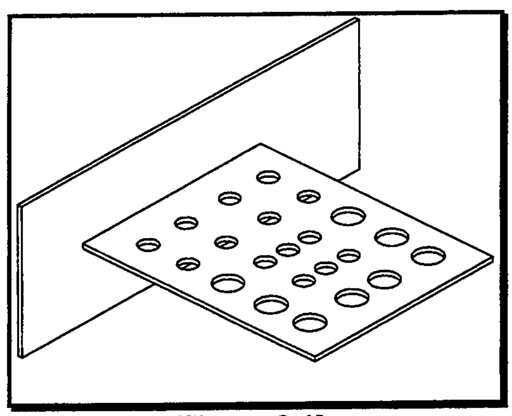

Figure 3.1b
Constant-Thickness Plate

Contoured Plate

Figure 3.1c shows a plate structure which has been contoured so that it varies in thickness over the area. For a metal plate this is typically done by computer numerically controlled (CNC) machining down from a constant-thickness piece of stock. For composites a constant-thickness plate could be CNC machined, but more typically the ply layup schedule is arranged so that the desired contour will be achieved without machining. If composite materials are used, the discussion in Section 2.5 may be relevant.

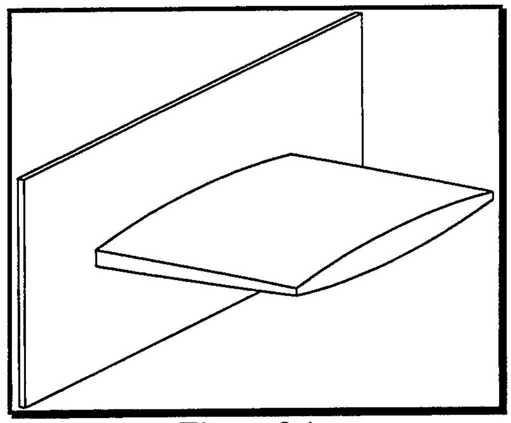

Figure 3.1c
Contoured Plate Structure

3.2 Beam/Spar/Pod Construction

This section initially presents an extensive discussion of the parameters associated with designing flutter model spars and spar networks. The final portion of this section describes the different methods for modeling the external contour of each flutter model section ("pod").

Individual Spar Parameters

As a general rule it is recommended that metals be considered first when attempting a flutter model spar design. However, a high GK/EI ratio, stiffness changing drastically over the length of the spar, or weight considerations may make it impractical to use metal in certain instances. In these cases composites should be considered. Generally the safest approach is to use fabrics. If the individual ply thickness is a small percentage of the average distance from the spar neutral axis and the total ply buildup, and if symmetric layups with alternating ply orientations are used, many of the potential problems associated with composites can be avoided. Often this approach will allow the composite to be treated as a pseudo-homogeneous material. For example, a graphite layup with 33% of the plys at a ±45° orientation and 67% of the plys at a 0-90° orientation (alternating between ±45° and 0-90°) will result in a layup whose material and strength properties can be predicted by weighting the values shown in the material properties table. (i.e. $E_{layup} = .33(3.8 \times 10^6) + .67(10.5 \times 10^6) = 8.3 \times 10^6\ psi$)

The following paragraphs describe some of the basic design considerations and options available when trying to design a particular spar or beam element to match bending and torsional stiffness requirements. The choices of material and the specific geometric configurations available provide a fairly extensive matrix of options. It is often possible to meet the target stiffness distributions with a variety of spar designs, with the choice of which is most appropriate often determined by weight, stress, or ease of fabrication considerations. The following sections present formulas for flanged rectangular spars, which are the most common spar configurations used in flutter models. The formulas defining the area moments of inertia for bending and torsional stiffness constants for a wide variety of other simple and complex geometric shapes can be found in standard textbooks such as Roark's Formulas for Stress and Strain by W. C. Young.

Geometric Shape of Main Element

The geometric shape of the main spar element is usually determined by the desired torsion to bending ratio, space envelope restrictions, and ease of fabrication. For a solid rectangular cross section of dimensions "a" and "b" (where "a" > "b") the stiffnesses are determined by the following relationships:

$EI_1 = (E\ a\ b^3)/12$ *Equation 3.2a*

$EI_2 = (E\ b\ a^3)/12$ *Equation 3.2b*

$GK = a\ b^3\ (1/3 - .21(b/a)(1 - ((b/a)^4)/12))$ *Equation 3.2c*

By varying the relationship between "a" and "b" it is often possible to match both bending target stiffnesses, or one bending and torsion. It is normally **not** possible to match all three at the same time without using some of the additional design variations discussed in the following sections.

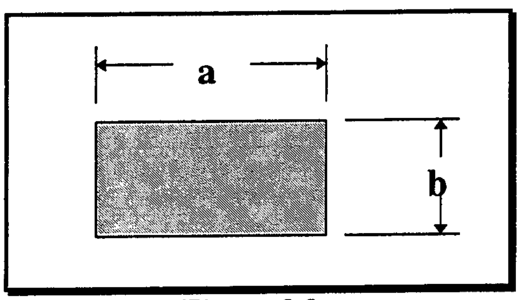

Figure 3.2a
Rectangular Cross-Section

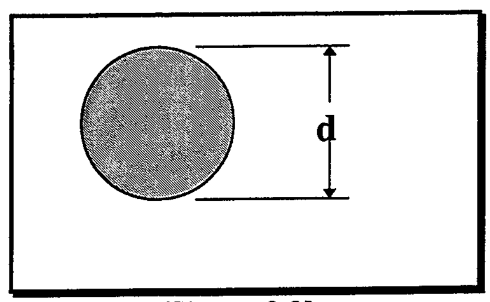

Figure 3.2b
Circular Cross-Section

In cases where the target GK/EI ratio is higher than can be achieved with a rectangular cross section, a circular cross section can be tried. The stiffnesses for a circular cross section of diameter "d" are determined by the following relationships:

$EI_1 = EI_2 = 3.1416\ d^4/64$ *Equation 3.2d*

$GK = 2\ EI = 3.1416\ d^4/32$ *Equation 3.2e*

Other geometric shapes are occasionally used. For high GK/EI ratios an ellipsoidal cross section may be a viable alternative when the envelope restrictions will not allow a circular cross section, or when it is desired to have the bending stiffness in one direction significantly different than the other.

Solid vs. Hollow

The formulas given in the previous section were for cross sections which are solid. Because the material furthest away from the neutral axis of the spar is most effective in determining the overall stiffness, hollow spars are often constructed to eliminate unnecessary weight. A second reason for using hollow spars is that it often allows alternate relatively inexpensive fabrication techniques (such as sheet metal bending and composite layups) to be used. The stiffnesses of a hollow circular cross section of outer diameter "d1" and inner diameter "d2" are defined by the following:

$$EI_1 = EI_2 = \pi\,(d1^4 - d2^4)/64 \qquad \textit{Equation 3.2f}$$
$$GK = 2\,EI = \pi\,(d1^4 - d2^4)/32 \qquad \textit{Equation 3.2g}$$

The stiffnesses of a hollow rectangular cross section with outside dimensions "a" and "b" (where "a" > "b") and a constant wall thickness "t" are defined by the following:

$$EI_1 = (1/12)(a\,b^3 - (a-2t)(b-2t)^3) \qquad \textit{Equation 3.2h}$$
$$EI_2 = (1/12)(b\,a^3 - (b-2t)(a-2t)^3) \qquad \textit{Equation 3.2i}$$
$$GK = (2t(a-t)^2(b-t)^2)/(a + b - 2t) \qquad \textit{Equation 3.2j}$$

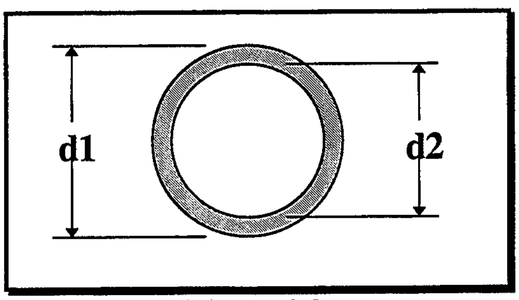

Figure 3.2c
Hollow Circular Cross Section

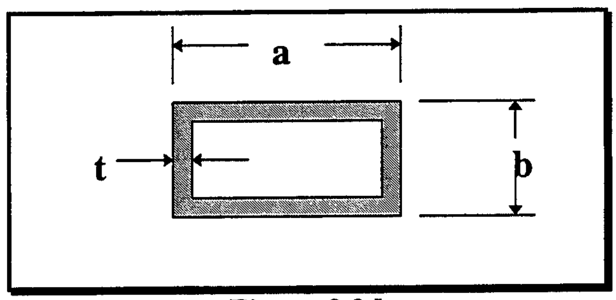

Figure 3.2d
Hollow Rectangular Cross-Section

The equations above assume that the no local buckling takes place, an assumption which is normally valid unless the wall thickness is extremely thin. A hollow spar design like that shown in the above figure may pose some problems for construction, however. If constructed from sheet metal or a constant thickness composite layup in two halves, joints become a concern. For stress reasons and to adequately transfer strains a relatively large overlap region is preferable. If two "U-shaped" halves are joined together the wall thickness on the sides will not be the same as on the top and the bottom, and the above formulas are not applicable. The formulas for the case where the side and top/bottom thickness are different can be found in <u>Roark's Formulas for Stress and Strain</u> . The formulas presented here were chosen because they are more applicable to the flanged spar designs discussed in the following section.

Flanges

The addition of flanges to the basic geometric shape of the spar element adds a great deal of flexibility for matching widely varying target stiffness distributions. Flanges can be used to significantly increase the bending stiffness in one direction while adding very little to the other bending or torsional stiffnesses. This allows the following general design process to quickly iterate to a solution:

- Match the lower of the two bending stiffnesses (EI_1) and the torsional stiffness (GK) using the formulas for the central section of the spar only
- Compute the bending stiffness in the other direction (EI_2) resulting from the central section of the spar
- Add flanges to raise EI_2 up to the higher target value
- Calculate the additional contribution to EI_1 and GK due to the flanges to confirm that they are negligible. (If not negligible, then iterate through the process again after reducing the target EI_1 and GK values by the calculated flange contributions.)

The following formulas define the contribution of the flange to the stiffness in each direction. It should be noted that "t" is defined as being half the flange thickness. This is consistent with the common method of fabricating hollow spars in upper and lower halves, and bonding them together along the centerline of the flange.

$$EI_1 = (E(c-a)(2t)^3)/12 \quad \textit{Equation 3.2k}$$
$$EI_2 = (E(2t)(c^3 - a^3))/12 \quad \textit{Equation 3.2l}$$
$$GK = (c-a)(2t)^3(1/3 - .21(b/a)(1 - ((b/a)^4)/12)) \quad \textit{Equation 3.2m}$$

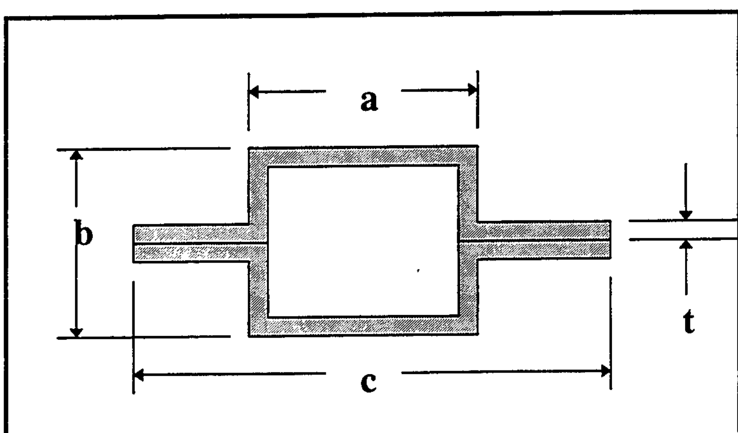

Figure 3.2e
Hollow Flanged Rectangular Cross-Section

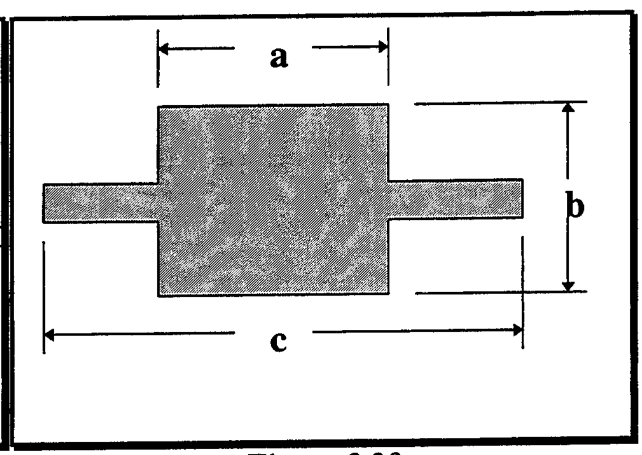

Figure 3.2f
Solid Flanged Rectangular Cross-Section

Note that the formulas and figures presented thus far all assume that dimension "a" is greater than "b". It is possible to obtain a configuration which looks like the following figure. In this case the height "b" is greater than "a". To properly calculate the torsional stiffness the "a" in the GK formula for the central "box" must refer to the longer side.

It should also be noted that it will not always be possible to match particular target GK/EI ratios even when flanged spars are used. The discussion at the bottom of the following page under the heading "High and Low Torsion to Bending Ratio Designs" presents a few alternatives which can be considered in the case of extremely high or low GK/EI ratios.

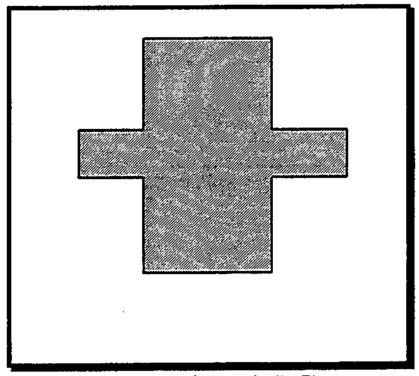

Figure 3.2g Special Case for Flanged Cross-Section

Constant Section vs. Tapering (Overall Dimensions or Wall Thickness)

The formulas presented define the stiffnesses of the spar at a particular cross section. Although occasionally a spar will have constant target stiffnesses over the entire length, it is more typical that the distributions will vary over the length of the spar. Matching of the target stiffness distributions will thus require that the cross section of the spar vary along its' length. Usually the target EI_1, EI_2, and GK values are determined at a series of discrete stations, the spar cross section is designed at each of these points, and the spar dimensions are transitioned between them. This results in a spar which will taper between adjacent sections.

If all the target stiffnesses are getting smaller in one direction along the spar, then the spar may taper smaller for all the defining dimensions. However, depending on how the stiffness ratios vary, it is also possible for the spar to have some dimensions which are increasing while others are decreasing.

It is also possible to vary the wall thickness "t" between adjacent sections. This might be done for a composite spar by gradually dropping off or adding plys to the overall layup. The load path should be carefully evaluated whenever this is done.

Whenever a varying stiffness distribution is being approximated by matching the design at discrete locations, care must be taken to evaluate what happens between the design stations. It is possible to accurately match the target distributions at discrete points and still have a very poor spar design. As an example, assume all three stiffness distributions vary linearly over the length of a rectangular spar from some nominal value at the root to zero at the tip. If the root stiffness values were used to define spar dimensions "a" and "b", and then these dimensions were straight line tapered to zero at the tip, a spar having dimensions of "a/2" and "b/2" at the midspan point will result. Using the formulas for a rectangular cross section, the resulting bending stiffness at the midspan would only be 1/16 of the root stiffness -- which is considerably less than the 1/2 root stiffness target. Increasing the number of design points will reduce the error, but the areas of the spar between each design point will still be low in stiffness. A good check of a spar design is to calculate an average overall effective stiffness for the spar and compare that with a similar calculation based on target stiffnesses.

High and Low Torsion to Bending Ratio Designs

With the use of hollow circular spar cross sections and composite layups employing primarily $\pm 45°$ ply orientations, it is possible to match GK/EI ratios not attainable with metal spars designed using the equations presented in the previous sections. Before the widespread use of composites, various designs for high GK/EI ratio metal spars were developed. One of these is illustrated in **Figure 3.2g**. These are often relatively expensive designs because they require extensive machining with numerous thin web sections. The designs illustrated are also not conducive to fabrication with composites.

Occasionally the opposite problem presents itself. When it is desired to match bending stiffness in two directions with a very low torsional stiffness, spar cross sections employing multiple thin flanges can be used. **Figure 3.2h** illustrates one example of such a cross section.

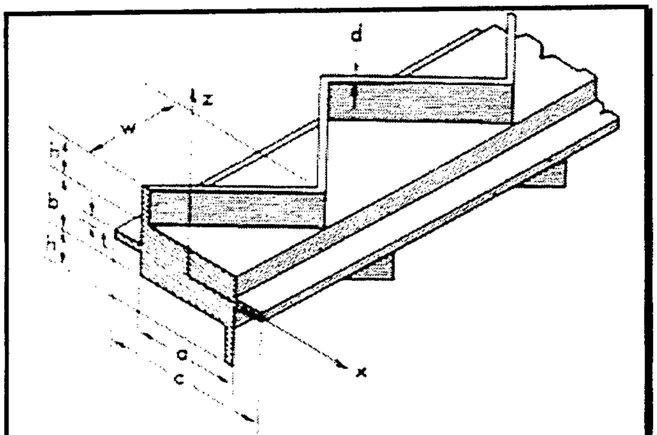

Figure 3.2g
High Torsional Stiffness Cross-Section

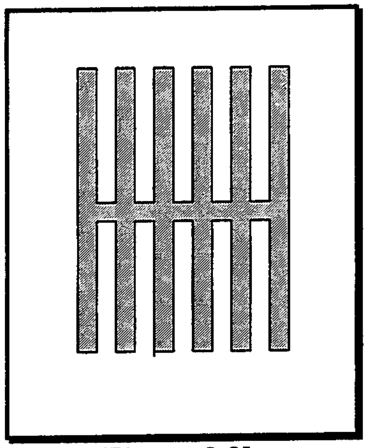

Figure 3.2h
Low Torsional Stiffness Cross-Section

Built-Up Spar Structures

Individual spar elements can be combined in various ways to match the stiffness distributions for more complicated structures such as delta wing configuration aircraft. The following sub-sections highlight how this is done for a few basic approaches.

Two-Spar Torque-Tube Structure

Another type of structural arrangement in which the spar structure provides the entire stiffness requirements is the two-spar torque-tube structure shown in **Figure 3.2i**. The two spars provide the bending stiffness EI, whereas the torque tubes increase the torsional stiffness GK to the desired value. This structure cannot simply simulate a fore-and-aft bending stiffness distribution. It does, however, provide a differential-bending type of stiffness, as will be shown later. The torque tubes are very stiff in bending and ensure that the general deflection of the structure at a spanwise station can be described as a deflection at the elastic axis plus a rotation about it.

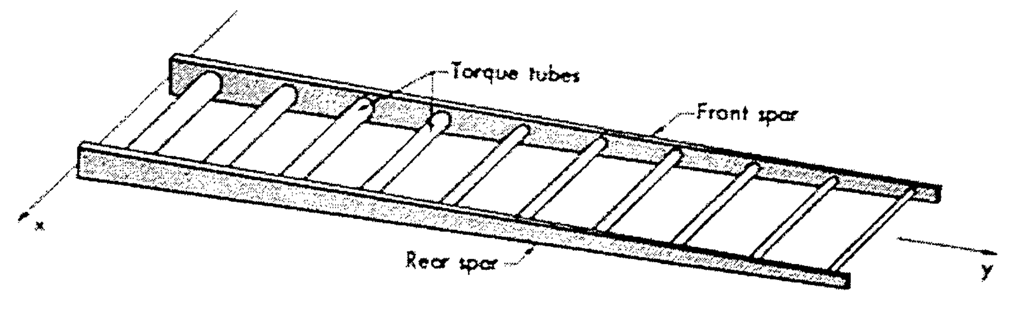

Figure 3.2i Two-Spar Torque-Tube Structure

Since the torque tubes are perpendicular to the spars and do not contribute to the bending stiffness EI, the sum of the bending stiffnesses of the front and rear spars must at each station equal the desired stiffness:

$$EI_{target} = EI_{spar1} + EI_{spar2} \qquad \textit{Equation 3.2n}$$

Also, the relative sizes and locations of the spars must be such as to ensure the correct location of the local elastic enters. With the concept that the elastic center at a given section is the point at which a load would have to be applied to produce pure bending if the local conditions extended over the whole span, it can be shown that the moment of the spar stiffness EI about the elastic center must be zero:

$$(dist1)EI_{spar1} + (dist2)EI_{spar2} = 0 \qquad \textit{Equation 3.2o}$$

Thus, Equation 3.2n and Equation 3.2o govern the spacing and bending stiffnesses of the spars.

To obtain the desired torsional stiffnesses for the model it is necessary to supplement the torsional stiffnesses of the spars by installing suitable torque tubes. In most models of this type the major portion of the torsional stiffness comes from the torque tubes. It is important to recognize, however, that on multispar models (as well as on multispar wings) the differential bending of the spars also contributes to the torsional stiffness, although in a complicated fashion. Even in the absence of connections between the spars they will offer some restraint to an applied torque. The torsional restraint set up by differential bending of the spars is a function of the second moment of bending stiffness about the elastic center and the third derivative of the twist. If we take into account the fact that when the wing twists the spars twist also, it is apparent that each spar offers an additional torsional restraint about the spanwise axis proportional to its own GK.

The three requirements of total bending stiffness and its first and second moments about the elastic axis generally cannot be satisfied by the use of two parallel spars. If the simulation of differential bending at each spanwise station is of secondary importance, its over-all effect can be represented approximately by a reasonable location of the two straight spars. If the correct simulation of differential bending is of primary importance, or if the other stiffness requirements are difficult to obtain with two straight spars, it may be desirable to add a third spar over at least a portion of the model span rather than resort to kinked or offset spars.

Beam Network

For low aspect-ratio lifting surfaces the flexibility in the chordwise direction is often of the same order of magnitude as in the spanwise direction. The modes for these structures cannot be expressed in terms of bending and torsion about a single axis. They are typically complex deflection surfaces which must be expressed in terms of a series of structural influence coefficients. Except for the most elementary of designs it is difficult to calculate a set of influence coefficients for a beam network. Typically a FEM will be required to iterate to an acceptable design. **Figure 3.2j** shows an example of a beam network structure used to simulate the influence coefficients of a delta wing.

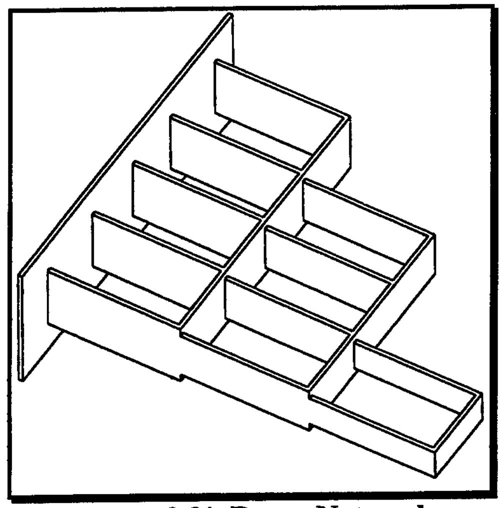

Figure 3.2j Beam Network Structure

Outer Contour Sections

It is usually necessary to represent the correct external shape for flutter model components to properly simulate the steady and unsteady airloads. As the internal support structure of the model deflects under these airloads, the external shell should also deflect without significantly changing the stiffness properties of the model. Each approach to simulating the external contour has its own advantages and disadvantages.

Solid Balsa or Rigid Foam

Solid balsa has been used extensively in many flutter models because it is easy to contour and has a relatively low density. For flat plate models the balsa can be oriented with the grain perpendicular to the plate to minimize the additional stiffness added to the structure by the balsa. It is common practice to use an adhesive bond over the entire plate to attach the balsa. One of the disadvantages of using balsa or any type of wood on a flutter model is that the wood can absorb moisture. This can cause the wood to swell, which may distort the structure. To avoid this balsa sections are usually sealed to prevent moisture absorption. Sometimes model airplane silk or a thin layer of fiberglass is added to the outside surface of the balsa.

For low speed flutter models with internal spars it is common to divide the external shell into separate segments - each of which is then attached to the spar at a single point to minimize the impact of the segment on the stiffness distribution. A thin metal "U" clip may be added to facilitate attachment to the spar. Streamwise gaps intentionally left between the segments to prevent load transference between adjacent pieces can be filled with a low density compressible foam or bridged with thin latex rubber sheeting. **Figure 3.2k** shows typical construction for a segmented external shell attached to an internal spar.

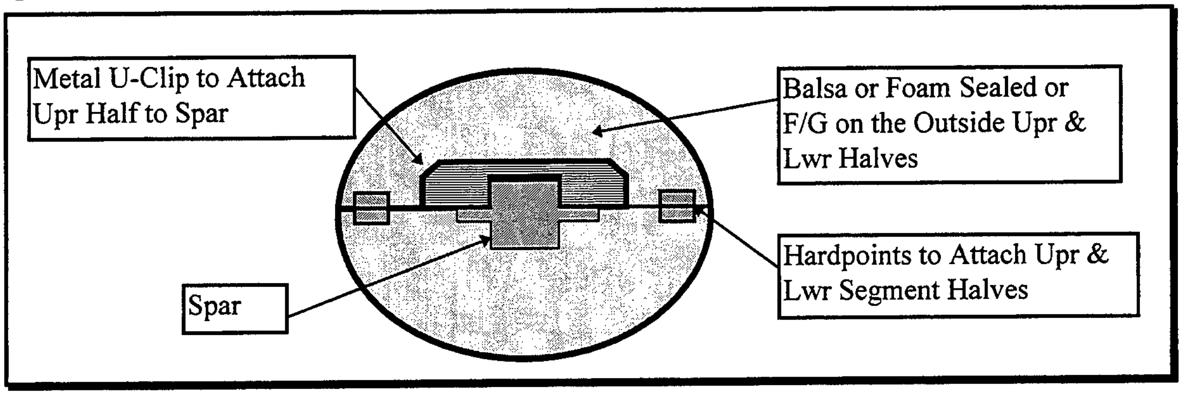

Figure 3.2k Fore/Aft View of Typical Segmented Construction

In some cases low density foam is used as an alternative to balsa. Because of the extremely porous and rough surface, an external layer of fiberglass or model ariplane silk is almost always added when foam is used.

Foam Sandwich or Egg-Crate Supported Skins

Foam sandwich or egg-crate supported skins can be used as an alternative to making solid segments of balsa or foam. Use of female wood molds allows fiberglass skins of the external contour to be laid up.

These skins can be kept relatively thin and lightweight using one of the following methods:
- incorporate balsa "egg-crate" support structure bonded to the inside surface of the skin
- make the outer skin a fiberglass/foam/fiberglass sandwich

In either case the internal support structure near the center of the segment typically includes a metal "u" clip to facilitate attachment to the spar. **Figure 3.21** shows a cross section of this type of construction.

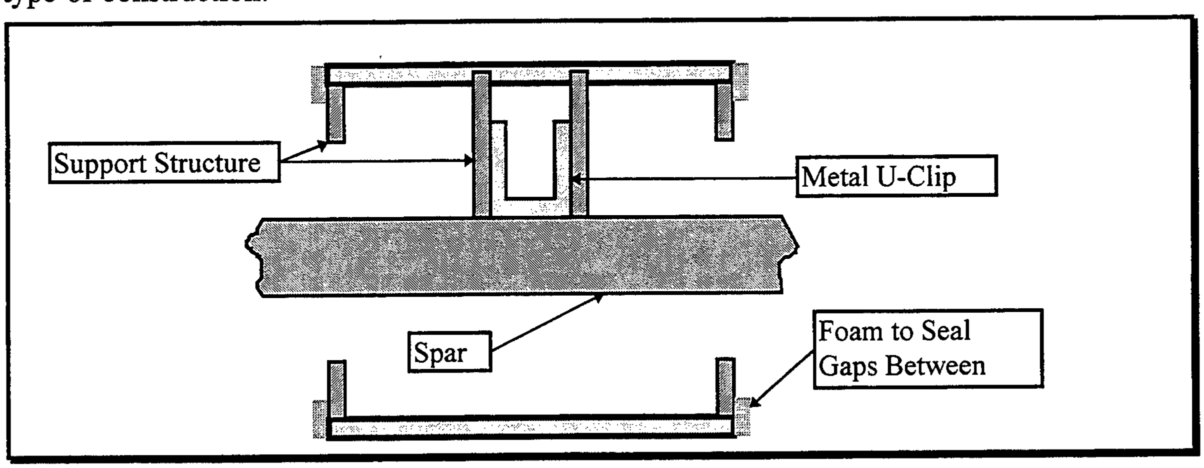

Figure 3.21 Side View of Typical Segmented Construction

Rubber, RTV, or Flexible Foam

To create a smooth external shell without gaps, very flexible materials are occasionally used. Ribs attached to internal spars can support thin latex sheets simulating the outer skin contour. Very little additional stiffness is added to the spars using this approach, but it is very difficult to control ballooning of the rubber skin above an airstream velocity of about ninety feet per second.

A flexible foam or an RTV material cured in molds can also be used to create the external shape on some flat plate and spar flutter models. A significant disadvantage to using rubber, RTV, or flexible foam on flutter models is that the damping of the model can be greatly increased. The availability of composites to create lightweight flutter components with smooth external surfaces has virtually eliminated the use of rubber in flutter model construction.

3.3 Stress Skin Construction

Because modern aircraft are being designed with more extensive use of composites and honeycomb sandwich structures which tend to be lighter weight, it is becoming more difficult to produce an adequately scaled flutter model without the use of similar construction techniques. The following paragraphs will cover some of the key design considerations when attempting stress skin construction of flutter model components. The sub-sections under Section 8.0 can be referenced for illustrative figures and a discussion of the design and analysis process used on a supersonic flutter model which employed stress skin construction.

Metal Skins

With the increasing use of fiberglass and graphite composites, metal skins are not often used in flutter models. The main reason for this is that it is very difficult to form metal skins into the complex contours found on many modern aircraft designs unless expensive molds and forming tools are used. However, metal skins have the advantage of being extremely predictable with regard to their material properties - and they provide an excellent external surface. Therefore, metal skins should at least be considered when the components involved have contours involving simple curves, or when then isotropic material properties present an advantage.

There are tradeoffs between the different design and fabrication considerations. Metal skins will occasionally still result in the best design. Aluminum and magnesium are the most common metals used for skins on flutter models.

Composite Skins

For the purposes of this paper composite skins will include discussion of graphite, fiberglass, and Kevlar. All of the materials are readily available and can be obtained as woven fabrics, unidirectional tapes, and roving. These materials can be pre-impregnated with resin, or they can be dry (for use in wet layups). Composite skins have the advantage of being relatively easy to form into the proper shape (as compared to metal skins).

Male patterns or female molds can be quickly fabricated from wood using CNC machining. Sometimes the wood molds or patterns are used directly for the process of laying up skins. At other times fiberglass female molds are laid up using a CNC machined male pattern. Female molds will maintain a better external surface finish and tighter control of external geometry than male patterns. Female molds are also frequently used as construction cradles for building up the structure inside the completed external skins.

The relative advantages and disadvantages of dry versus pre-impregnated materials must be weighed against the requirements of the particular flutter model and the experience of the individuals doing the fabrication. It is also possible to use a combination of the approaches. For some of the layups described in Section 8.0 the outer layer of the skin was a layer of dry fiberglass fabric which had a measured amount of resin added to it, and the remainder of the layup was pre-impregnated unidirectional graphite tape. The entire layup was cured together at an elevated temperature.

3.4 Replica Construction

Replica construction involves duplicating the construction methodology for the full-scale design when making the model. This involves properly representing all structural members including skins, spars, longerons, etc. Generally this approach cannot be followed exactly because of unequal scaling factors, mounting constraints, and the particular requirements of the planned testing. However, it is becoming increasingly common to start with the full-scale design and to make some simplifications and changes while maintaining the basic relationship of skin layups and the main structural members. The design of the components described in Section 8.0 followed this basic approach.

The previous discussions regarding stress skin and spars is generally applicable to replica construction. However, replica construction will typically require extensive use of finite element modeling since the assembled structures are usually too complicated to evaluate using handbook formulas.

3.5 Hinged Control Surfaces

Control surfaces on flutter models must be attached in some manner to the fuselage, main wing, or other structure. The hinges and bearings for the full scale design can be modeled with reduced-scale bearings and hinges, or with flexures. Usually the angular deflection and loading requirements for the control surfaces will determine which approach is used. Large angular deflections or actuated surfaces will usually require hinges or bearings. Relatively small angular deflections permit the use of flexures which have more predictable dynamic characteristics. Because flexures generally do not have sliding friction associated with the operation, the damping of a flexure attachment is much less than for a bearing or hinge, a very desirable characteristic for most flutter model applications. The following three sections present a brief discussion of the most common approaches for control surface attachment, and some of the critical design considerations.

Hinge and Bearing Attachments

For flutter models which incorporate actuated surfaces or large angular deflections it is often necessary to use hinges or bearings. The disadvantage of using hinges or bearings is that the friction and damping characteristics associated with these attachments must be evaluated and accounted for. Some of the factors which can significantly effect the friction and damping characteristics of hinges and bearings include:

- the difference between static friction and dynamic friction
- galling of similar materials
- differential thermal expansion of dissimilar materials
- wear of close-fitting moving parts
- vibration between close-fitting moving parts
- slight changes in alignment when parts are interchanged
- the effects of cleaners, lubricants, dirt, and dust

With hinges and bearings it is difficult to ensure that the frictional and damping characteristics of the attachment will remain constant under all circumstances. The hardware generally undergoes repeated model changes, experiences wear, and may be tested at different temperatures. The items listed above must be given due consideration, and any differences between the calibration setup and the tunnel installation taken into account. This is particularly true for simple pin-type hinges. Precision bearings properly installed will generally give more consistent results.

It is also desirable to eliminate "slop" or "free-play" in the system. With bearings and hinges this usually results in a "design tradeoff", because rotating attachments which are tight enough to have no "free-play" will tend to have increased friction and damping.

Simple Beam Flexures

In certain cases simple beam flexures are used to simulate a hinge or bearing attachment. This is usually done when the anticipated deflections across the attachment are very small (i.e., if the target rotational spring rate is relatively high compared to the structure on either side). Standard beam formulas can be used to design these flexures and these formulas will give very predictable results when properly applied. However, the "back-up stiffness" of the structure to which the flexure is attached should be evaluated to see it this needs to be treated as another spring in series.

In cases where the anticipated deflections are somewhat larger, then the vertical/horizontal translation deflections of the beam inherently associated with a rotation may introduce undesirable modal characteristics. In these cases an alternate flexure arrangement should be considered.

X-Type Flexures

An X-type flexure is an assembly of two crossed beam elements usually oriented perpendicular to each other. X-type flexures are used extensively in flutter models because they behave kinematically much more like a hinge or bearing than a single beam element, yet they retain the low damping characteristics of a flexure. The rotation point of an X-type flexure moves very little over relatively large angles. The vertical and horizontal translational stiffness of an X-type flexure can be kept relatively large compared to the rotational stiffness.

X-type flexures are typically made in two separate halves for ease of fabrication. Stainless steel is the most common material -- although X-type flexures for flutter models have occasionally been fabricated from aluminum, plastic, or composites. For metal flexures wire electric discharge machining (EDM) is an efficient means of fabrication. **Figure 3.5a** shows one half of an X-type flexure assembly. The figure shows sharp inside corners, but it is standard practice to include a radius on the actual hardware to reduce stress concentrations. Standard formulas for stress can be used to check whether a particular flexure design will have adequate factors of safety. Fatigue is a potential failure mode and may need to be evaluated, particularly if aluminum or other materials which exhibit poor fatigue characteristics are used.

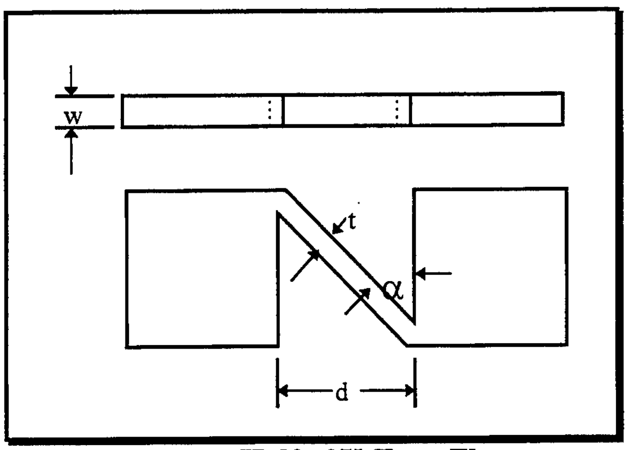

Figure 3.5a Half of X-Type Flexure

If the desired rotational stiffness "k" (in-lb/rad) is known, and the angle "α", length "d" (inches), width "w" (inches), and modulus of elasticity "E"(psi) are assumed, then Equation 3.5 can be used to obtain the required thickness "t" for an X-type flexure. This equation was derived based on superposition of simple beam formulas, and is therefore subject to similar restrictions. (e.g., the individual flexure width "w" should be significantly less than "d", and should be of the same order of magnitude as the thickness "t".)

$$t = [(6kd)/(wE(\sin\alpha))]^{1/3} \qquad \textit{Equation 3.5}$$

Figure 3.5b shows two halves of an X-type flexure assembled together in their final orientation. It is a good practice to make the attachment areas of the flexure at least one order of magnitude stiffer than the target springrate for the flexure. It is also advisable to design the flexures slightly overstiff – and then "tune" them down to the required value during calibration of the hardware.

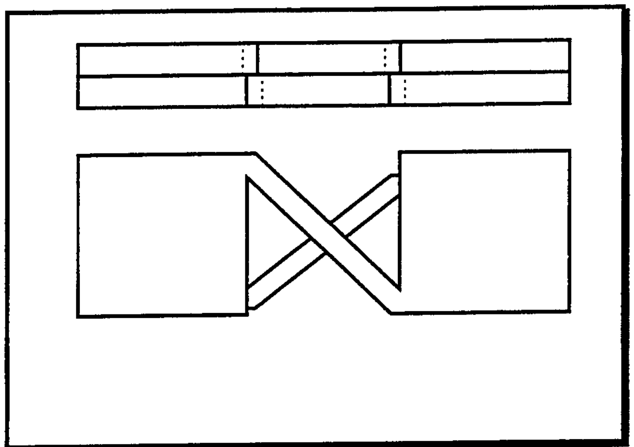

Figure 3.5b Assembled X-Type Flexure

4.0 INSTRUMENTATION

Instrumentation on flutter models may be added for any of the following reasons:

- to monitor loads at critical points in the model structure
- to help identify the modal patterns associated with particular components of the model
- to help identify phasing and relationships between the motions of different components
- to help identify shock locations and other aspects of the unsteady aerodynamics

The following three sections briefly discuss the most common types of instrumentation included on flutter models.

4.1 Strain Gage Bridges

Full strain gage bridges are often added to flutter model spars to monitor loads. The same gage output can also be used to determine the phasing for modal deflections. For stress skin structures gaging can be added directly to critical points on the component surface.

Sometimes strain gages are added to other elements such as the cross beam members in a X-type flexure. In these cases a half bridge is sometimes used because of space limitations. These bridges can be used to measure loads, but often they only provide the phasing for the rigid body modes of the control surface attached to the flexures.

4.2 Accelerometers

Accelerometers are frequently mounted at various locations within the flutter model structure to identify modal patterns and provide quantitative data for the motions. The positions of the accelerometers are usually chosen based on the anticipated mode shapes for the structure. For wing and control surface components the accelerometers are normally positioned to measure the acceleration perpendicular to the reference plane of the surface. For fuselage sections, nacelles, and other structures which may have significant motion in multiple directions, several accelerometers are often located close together with the measurement planes oriented orthogonal to each other.

4.3 Dynamic Pressure Transducers and Piezoelectric Strain Elements

Occasionally high speed stress skin flutter models will have dynamic pressure transducers located at various positions in the external skin contour. These transducers can be used to obtain quantitative pressure data which may be useful in identifying the location of the oscillating shock wave associated with some high speed flutter mechanisms.

Piezoelectric strain elements are currently being investigated for their usefulness on flutter models. These elements can be used as transducers to measure the direction and magnitudes of strains at particular locations. These elements can also have a voltage applied to them so that a strain is induced into the flutter model structure at specific locations. This application can be used to excite or modify the modal dynamics of a particular component.

5.0 MODEL CALIBRATION TECHNIQUES AND "TUNING"

The information contained in this section addresses the most common calibration techniques used to measure the properties of samples and final flutter model hardware. Calibration is necessary because relatively small deviations in weight, machining tolerances, material properties, and a host of other variables can sometimes result in significant deviations from the original targets. These deviations can often be corrected for by "tuning" the final hardware.

5.1 Stiffness

Two methods are frequently used for measuring the stiffness distribution of flutter model components. The "mirror calibration" technique is a very efficient approach for spars and high aspect ratio elements. For low aspect surfaces which do not exhibit "beam-like" deflections it is usually necessary to use an approach involving structural influence coefficients.

"Mirror" Deflections

A convenient method for measuring the bending or torsional stiffness of a flutter model component which acts primarily like a beam is illustrated in **Figures 5.1.a** and **5.1.b**. To obtain the stiffness between any two adjacent mirrors the following formulas were derived from basic beam formulas using small angle approximations. In addition to the variables indicated in the figures, "d" = distance between mirrors 1 & 2, and "A" = distance from the mirror closest to load and the load application point.

Bending:

$$\theta/\# = (\Delta Z_{\text{mirror }1} - \Delta Z_{\text{mirror }2})/2LP \qquad \textit{Equation 5.1.a}$$

$$EI = 1/(\theta/\#)[(d^2/2) + A(d)] \qquad \textit{Equation 5.1.b}$$

Torsion:

$$\theta = (\Delta Y_{\text{mirror }1} - \Delta Y_{\text{mirror }2})/2L \qquad \textit{Equation 5.1.c}$$

$$GJ = d(M)/\theta \qquad \textit{Equation 5.1.d}$$

Influence Coefficients

An alternate method for obtaining stiffness information is to place a distribution of load/measurement points on the component surface. If point loads are applied at each of these locations, and the deflection is measured at each location using a coordinate measuring machine or dial indicators, then it is possible to develop a set of structural influence coefficients defining the stiffness distribution for the component. A detailed treatment of this approach is beyond the scope of this paper, but the methodology can be found in any standard text dealing with complex structures. This approach for obtaining stiffness data is most applicable for delta wings or other structures which behave in a manner where the formulas derived from beam theory are not valid.

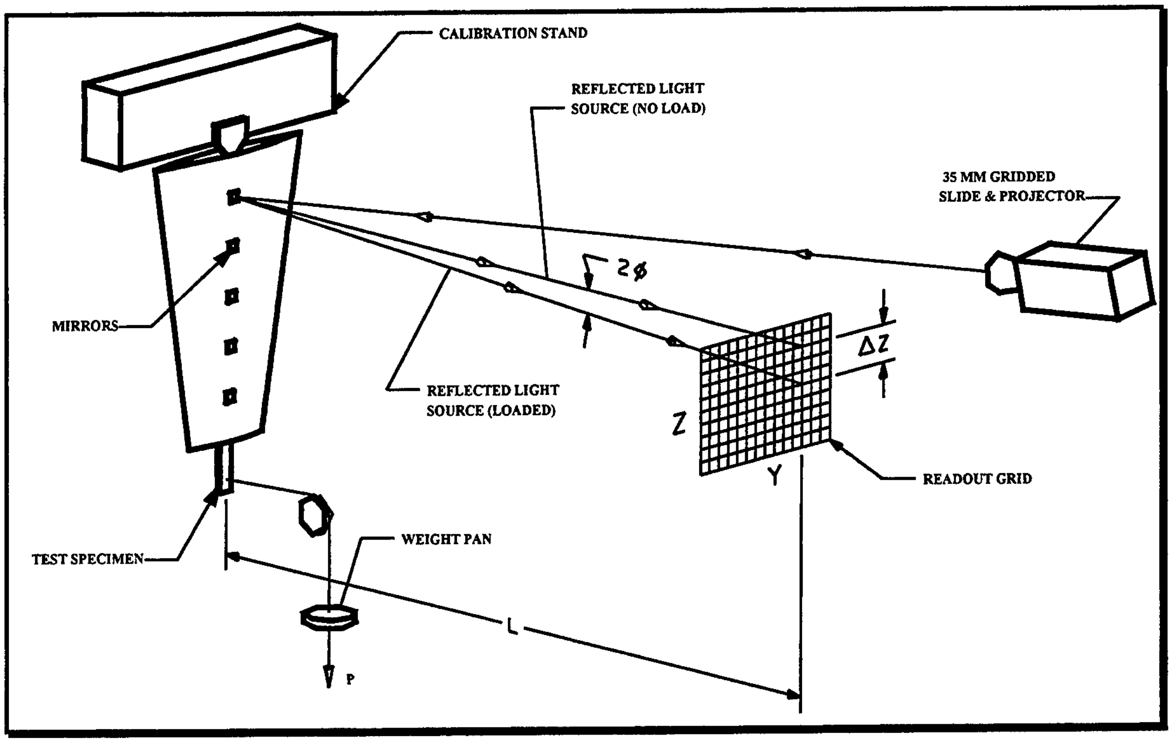

Figure 5.1.a Typical Setup For Measuring Bending Stiffness

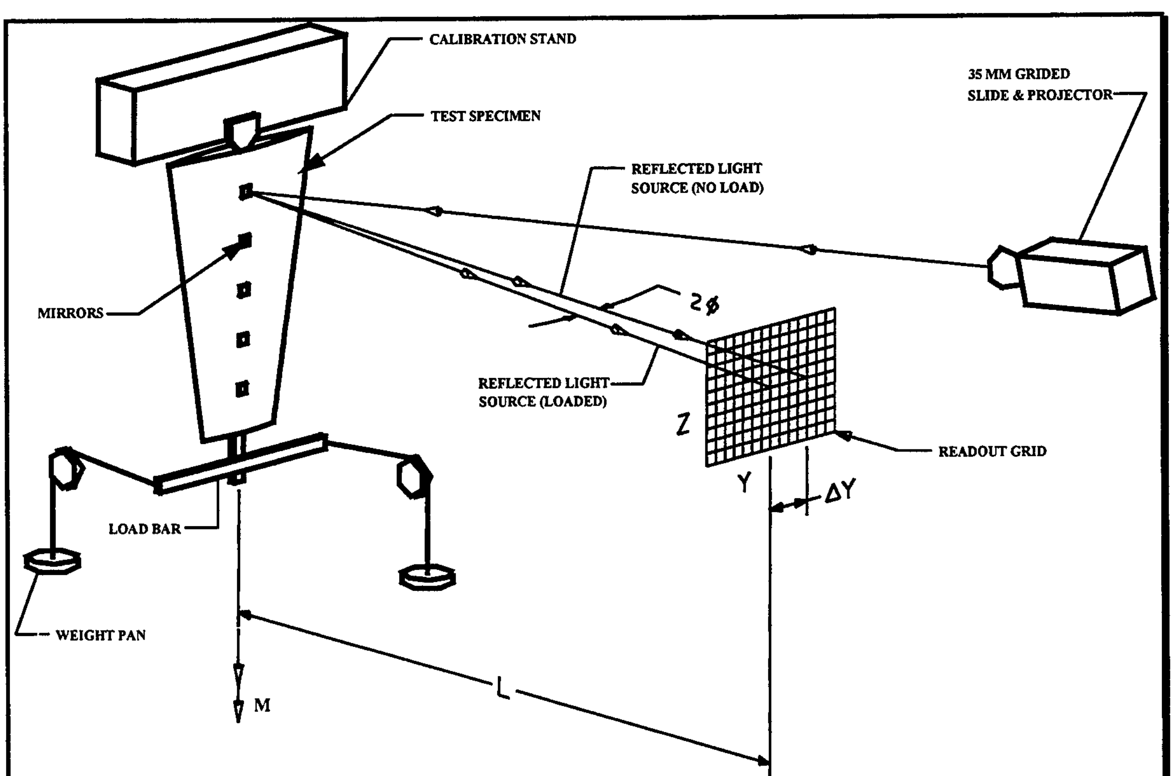

Figure 5.1.b Typical Setup For Measuring Torsional Stiffness

5.2 Mass and Inertia Properties

Overall Mass and CG Determinations

Scales are employed to measure the mass of individual components. Electronic scales covering a variety of ranges can allow this data to be taken quickly, even when there is a large number of individual components.

Locating the center of gravity (CG) can be done in a number of ways. The part can be balanced on a knife-edge and the line formed by the edge is marked. If this is done with the knife-edge in several orientations the intersecting lines will locate the CG.

Sometimes parts can be suspended from one corner so that they hang freely. A plumb line hanging down from the same point will cross over the CG. If the process is repeated with the part hung from several different points, the intersection of the plumb line markings will locate the CG.

The previous two methods will give the required accuracy if done carefully. However, they are rather tedious and can require a significant amount of time if there is a large number of parts. Parts with rapidly curving surfaces and unusual shapes may also make these methods more difficult in practice.

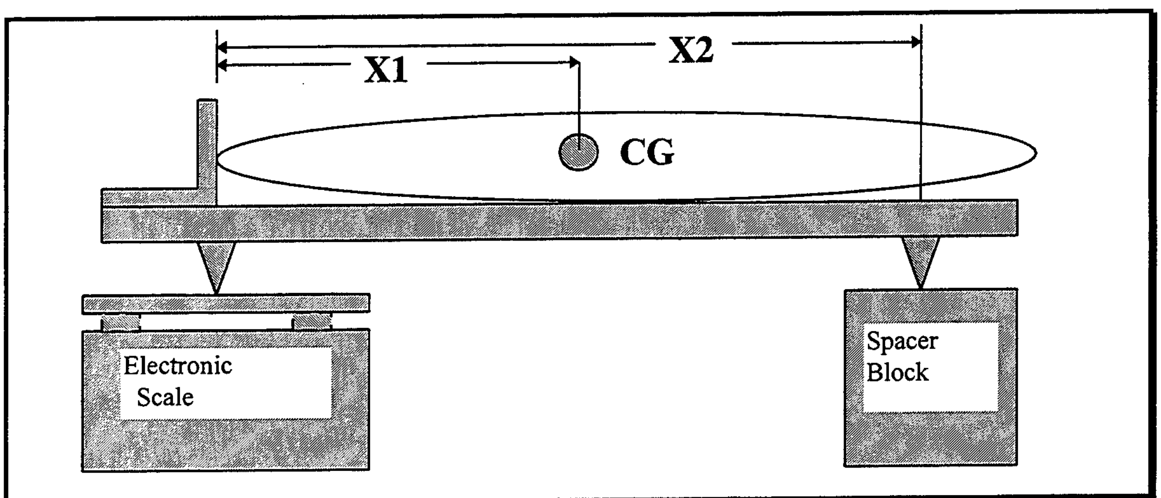

Figure 5.2a Setup For Determining CG Location Using an Electronic Scale

An alternate method is to use a fixture such as the one illustrated in **Figure 5.2a**. If the part has weight "W1", the scale reading "W2"can be used to determine how far from the vertical stop the CG is located. (Reference equation 5.2a.) By orienting the part in two directions the CG can be located from two different edges or corners. This procedure is very efficient for doing large numbers of parts, and the CG location is typically repeatable within .020".

$$X1 = X2(1 - W2/W1) \qquad \textit{Equation 5.2a}$$

Measured Mass Moments of Inertia

There are a number of methods for experimentally measuring the mass moments of inertia for individual flutter model components or built-up assemblies. The most common method is to use some variation of a torsional pendulum. Torsional pendulums typically have a lightweight beam or platform suspended from wires or cables. The pendulum can be made to rotate about a vertical axis in an oscillating fashion. The frequency of oscillation is dependent on the effective torsional stiffness "K" resulting from the cables, the inertia of the beam or platform about the rotation axis, and the inertia of any object attached to the pendulum. The following equation allows the mass moment of inertia about an object's CG to be determined if the period is known. The period for one cycle can be determined by counting a reasonable number of cycles (i.e. 10 to 50) and timing with a stopwatch. A strobe light may prove useful in cases where the period is too short to effectively use the stop watch.

$$I_{object} = K(Mass_{pendulum} + Mass_{object})(period)^2 - I_{pendulum} \qquad \textit{Equation 5.2b}$$

Figures 5.2b and **5.2c** depict bi-filar and tri-filar pendulums respectively, the most commonly used configurations.

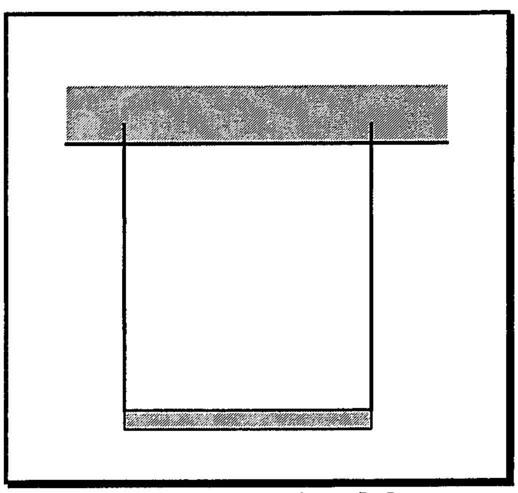

Figure 5.2b Bi-Filar Pendulum

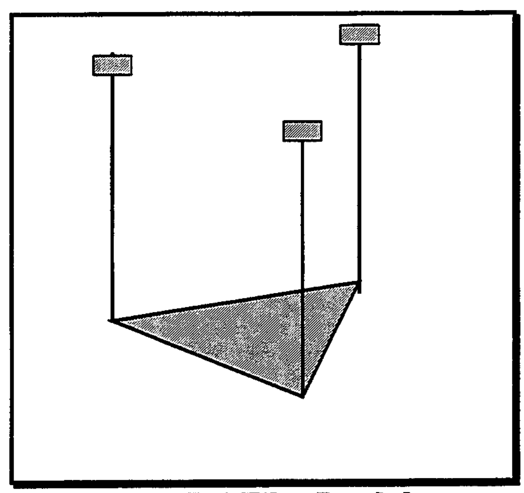

Figure 5.2c Tri-Filar Pendulum

Tri-filar pendulums are generally more convenient to use because objects can often be placed directly on the triangular platform with no special provision for support. Occasionally the object is large enough that it cannot be positioned between the wires so that the CG of the object is located on the rotation axis of the pendulum. In these cases the object can sometimes be attached to the bottom of the pendulum using tape. However, care must be taken to ensure that the object moves rigidly with the platform, otherwise the measurements will not be accurate.

The accuracy of the measurement is directly related to the magnitude of the inertia being measured in comparison to the pendulum inertia. Therefore it is common to have pendulums of multiple sizes to optimize accuracy. A bi-filar is generally used when the component being measured is extremely lightweight. For a bi-filar with a beam of length "D" and cables of length "L" the torsional constant can be approximated using the following relationship ("g" is the acceleration due to gravity):

$$K_{bifilar} \approx (D^2 g)/(16\pi^2 L) \qquad \textit{Equation 5.2c}$$

Equation 5.2c is not valid for tri-filars, and it should only be used as an approximation for bi-filars. The normal procedure for both bi-filars and trifilars is to calibrate them using bars, disks, or other shapes for which the mass moment of inertia can be accurately calculated. After recording the pendulum's period for each of two objects of a known mass and inertia, equation 5.2b can be used to solve for the two unknowns, "K" and "$I_{pendulum}$". It is usually a good practice to perform the calibration using objects of very similar mass to that of the components to be measured. Depending on the particular wires or cables used for the pendulum the torsional constant "K" can vary slightly as a function of the combined mass of the pendulum and object being measured.

It is also important that the object's CG be placed on the pendulum's rotation axis with reasonable accuracy. If it is placed significantly "off-center" this may induce swinging of the pendulum. Any significant motion other than pure rotation can impact the accuracy of the measurement or calibration. Therefore it is normal practice to locate the component's CG as accurately as possible before measuring mass moment of inertia.

The mass of the air being moved by the object on the pendulum is normally negligible. However, in cases involving extremely lightweight surfaces it is occasionally desirable to try to account for the mass of air being moved. Sometimes this is done using a calculated value. However, it is also possible to construct a constant thickness flat plate of the same planform as the surface being measured. The difference between the calculated inertia of this flat plate and that determined for the flat plate using the pendulum will equal the contribution due to the air mass movement. This value can then be used to adjust the measure inertia of the original surface.

Sectioned Sample

For stress skin construction of small to medium sized components, making a sample part is often done to fine tune the design process. The sample part must be checked for stiffness, overall mass properties, and the dynamic data discussed in the following sections. After these tests, the sample is often cut up into small sections. The mass properties of the individual sections can then be measured, compared with design values, and adjustments made prior to fabricating the final part.

5.3 Mounting Options

When evaluating frequencies and mode shapes there are various options available with regard to how the data is taken. The following two sections briefly discuss some of the most basic considerations associated with evaluating individual components versus assemblies, and cantilevered versus free-free mounting.

Individual Components vs. Assemblies

The advantage of obtaining frequency and mode shape data for a single component is that the structure is usually relatively simple, and it is relatively easy to interpret the results for the isolated component. The disadvantage is that the mounting conditions and interactions with other components is usually neglected or must be idealized.

The advantage of obtaining frequency and mode shape data for an entire model assembly is that this represents how the hardware will be tested in the wind tunnel. Any interactions between various components will be reflected in the results. The disadvantage is that it is often very difficult to interpret the results and interactions between components from the assembly data alone.

For all but the simplest of flutter models a combination of these two approaches is usually employed. Dynamic data is taken for the individual components in isolation. Then major subassemblies are built up with additional data taken at each stage. Normally the quantity of data taken for each component diminishes as the assemblies are built up. An individual component will normally have extensive mapping of node lines for all the frequencies of interest. At the subassembly and overall model assembly stage the data is usually restricted to obtaining frequencies and just enough acceleration or node line information to identify the mode associated with each frequency.

Cantilevered vs. Free-free

In cases where a component or subassembly is attached at one or two points with a relatively rigid joint it will probably be best to test the individual component or subassembly bolted or clamped to a rigid massive block. The attachments in the analytical model should be locked out to simulate this case for comparison. A wing with a single spar with a mounting block at the root is an example of a component which is commonly cantilever mounted. One disadvantage of cantilever mounting a component is that the effect of mass properties in the mounting area will not have a significant impact on the dynamic measurement results. Showing a good correlation of the mass properties in this area may then be more important for the overall model/FEM correlation (reference Section 5.8).
In cases where the attachment of the individual component is through multiple attachments which have significant flexibility associated with them, cantilever mounting can give poor or misleading results. An example of this is a rudder attached at multiple hinge points with a separate actuator link. Locking out the attachment points in the analytical model is likely to drastically change the predicted frequencies and mode shapes. Although it may be possible to take measurements to compare against this analytical case, the correlation may not be a good indication of what will occur for the installed condition with flexible attachments. For cases like this it is generally better to suspend the component by rubber bands or bungee chords and compare the measurements against the analytical model of the component in a "free-free"

condition. Care should be taken to ensure that the attachment locations for the rubber bands or bungee chords do not significantly affect the modes. Attachments located on node lines are best. Dynamic data for the overall model assembly is normally done with the hardware suspended to simulate a free-free state. **Figure 5.3** shows a typical example of how a flutter model component can be suspended.

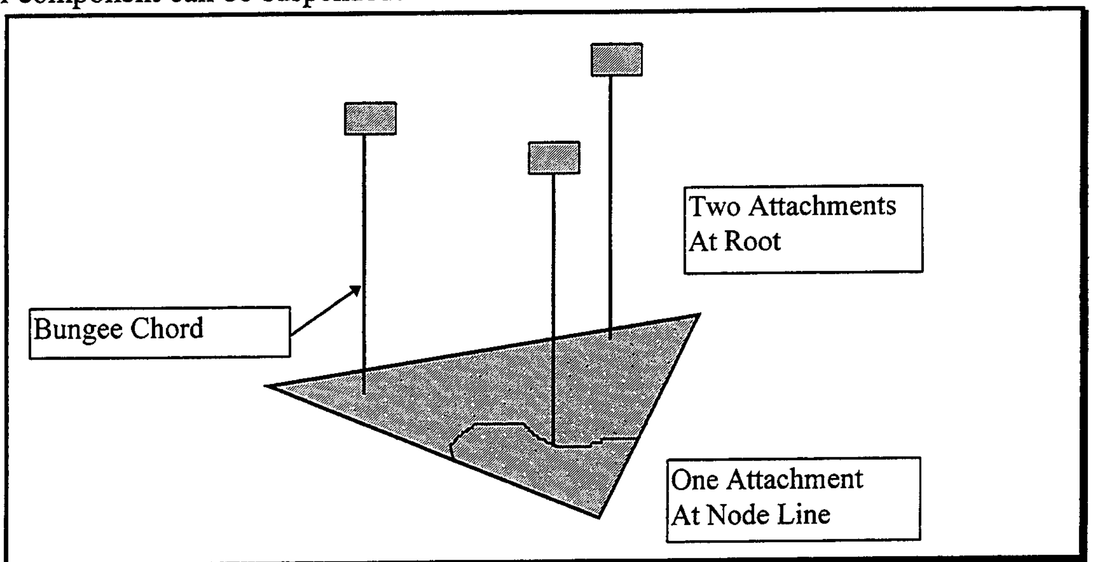

Figure 5.3 Typical Setup for Free-Free Testing

5.4 Natural Frequency Determination

For determining the natural frequencies of flutter model components a frequency analyzer is the most common instrumentation used. The capabilities and operation of specific frequency analyzers varies, but all are capable of taking the input from one or more accelerometers mounted on the component surface and displaying the data in various formats. There are various brands of wax which allow an accelerometer to be temporarily attached to the component surface.

In some cases there are accelerometers permanently installed within the structure for the component to be used during wind tunnel testing. Using the output from such an accelerometer has the advantage of not adding additional mass to the component being evaluated. The results will also be directly comparable to what will be obtained during tunnel testing. Even when this approach is used it is advisable to make a check with a "roving" accelerometer positioned at various points on the component to ensure that frequencies/modes are not missed because the accelerometer was inadvertently positioned directly on a node line.

"Rap" Test

The simplest method for exciting the natural frequencies of the structure being tested is to give it a "rap" with a small impact hammer or a finger. Some practice is usually necessary to avoid making double hits, keeping the output within the gains set on the analyzer, etc. This method can be used for cantilever or fee-free mounted structures, and it is often possible to get data within a few minutes.

Shaker Excitation

An alternate method for exciting the natural frequencies of the structure being tested is to mount the output rod from an electromagnetic shaker to the surface and drive it through the anticipated range of natural frequencies. The rod attached to the structure is normally lightweight, thin, and somewhat flexible in bending (e.g. a thin plastic rod or wooden dowel). Temporary attachment to the surface is usually done with a quick-drying epoxy adhesive which can be easily removed after the testing. This set up is illustrated in **Figure 5.4**. A combination of random input to get mode locations followed by sine dwell for verification works well.

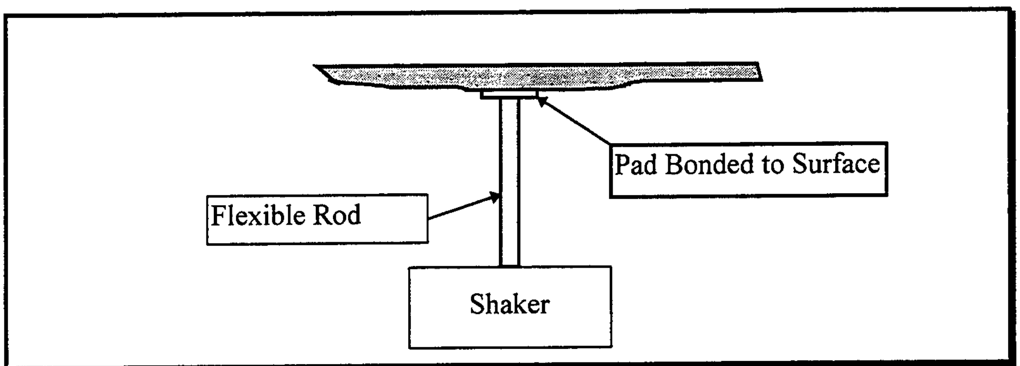

Figure 5.4 Shaker Attachment to Surface

5.5 Mode Shapes

"Mode shape" refers to the characteristic motion associated with a particular natural frequency of a structure. "Node lines" are lines going through points on the structure which undergo no motion during deflection of the component. "Node lines" are also defined as the areas where the phase of the surface motion reverses and passes through zero. **Figure 5.5** shows a node line for a structure undergoing bending.

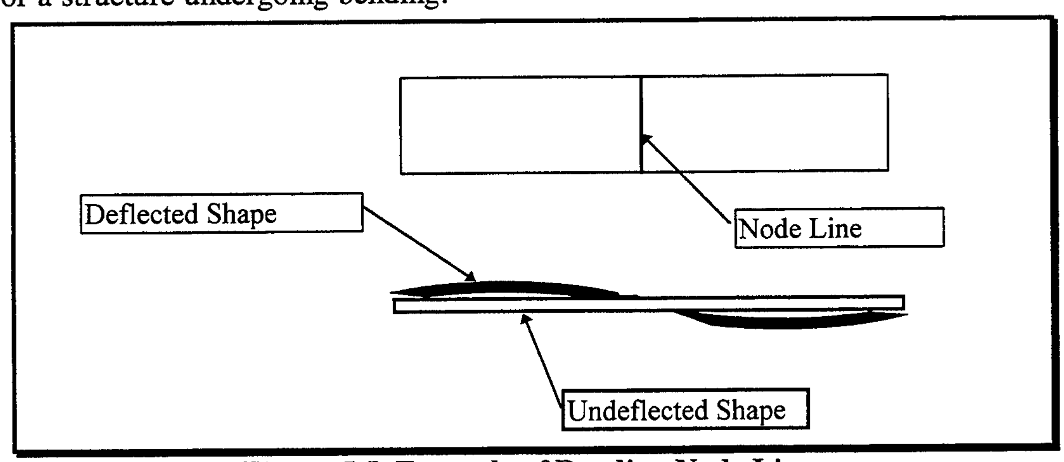

Figure 5.5 Example of Bending Node Lines

The following four sections describe methods used to locate node lines and identify the mode shapes of flutter model components.

Salt or Powder

For relatively flat surfaces such as delta wings it is sometimes possible to use salt, sawdust, or some type of powder to make node lines visible. The powder should be a color which contrasts with the surface being checked. The powder is scattered over the surface, which is then excited at one of the natural frequencies using an electromagnetic exciter. The powder will gradually be bounced away from areas of high motion and collect along node lines.

Although quite simple in principle, this method tends to be difficult to get accurate results from most situations.

Mapping with Impact Hammer

A common method for mapping node lines requires a frequency analyzer, an accelerometer mounted on the surface, and an "impact hammer" with an accelerometer in it. The method is briefly summarized below.

- Connect the output from the accelerometer attached to the surface to one data channel of the frequency analyzer
- Connect the output from the "impact hammer" to a second channel of the frequency analyzer
- Set the frequency analyzer to the desired frequency and display the phasing of the transfer function between the two channels of data (accelerometer & "impact hammer")
- Rap the surface with the "impact hammer" at points gradually moving across the surface - the points where the phasing passes through zero (reverses direction) correspond to a node line. These points can be marked with white-out or a wax pencil.

Although the above approach can be somewhat tedious, it requires a minimum of equipment and can give accurate results.

Accelerometer Grid

Sometimes a large number of accelerometers will be mounted to the external surface of a flutter model component (usually in a "grid" pattern) and an electromagnetic shaker used to excite a particular frequency. The acceleration data from each point on the grid where an accelerometer is located can be analyzed to give quantitative measurements of the surface motion. The main disadvantages of this approach are that the cost of the equipment necessary to obtain and analyze the data can be quite expensive. The weight of the accelerometer grid attached to the surface is also normally significant. This will change the frequencies. This effect must be taken into account analytically.

Laser Scanning

Laser scanning of a surface being excited at a particular frequency can give very good plots of deflections and node lines. This approach can give data similar to that obtained with an accelerometer grid. Laser scanning has the advantage of not introducing extra instrumentation mass to the component being tested. As the equipment used for this approach becomes more affordable it will probably be used more extensively.

5.6 Stiffness Tuning of Spars and Flexures

Spars and flexures are typically designed slightly "overstiff" because it is difficult to analytically account for all the variables involved with construction of a flutter model. It is normally easier to reduce the stiffness of a structural member than to increase it. When the stiffness or spring rate of a spar or flexure is initially measured using one of the techniques described in Section 5.1, there will invariably be some deviations from the theoretical targets. If the member has been designed "overstiff" some material can be removed by sanding, filing, or grinding the spar or flexure. Many times it is possible to do this while the component is still set up for the stiffness calibration.

For metal spars the material properties are very consistent, so it is generally only necessary to design the spar two or three percent overstiff. For composite spars and flexures where the machining tolerance is a significant fraction of the overall thickness, it may be necessary to design the component as much as five or ten percent overstiff.

5.7 Mass Ballasting

Although detailed weight spreadsheets and an accurately controlled process for preparing composite layups and applying adhesive can result in very accurate weight predictions, it is still advisable whenever possible to initially design the sections of a flutter model to be five to fifteen percent underweight. Based on the stiffness calibrations and the initial mass property determinations it is then possible to "tune" the mass properties of each section to achieve a better match with the target values.

The following list summarizes the procedure generally used for mass ballasting a single flutter model component:

- Take initial weight, CG, and mass inertia measurements as described in Section 5.3. Ideally the overall weight and mass inertia measurements will be less than the theoretical targets.
- Obtain multiple ballast weights (lead, tungsten, steel, etc.) equal to the difference between the target weight and the initial measure weight of the component.
- Position the ballast weights in or on the component so as to give the proper CG location.

- Check the mass inertia properties and adjust the positions to achieve the desired inertias (e.g. two or more identical weights moved equally outward from a single point can increase the mass moment of inertia without changing the overall weight or CG location).
- Permanently bond or attach the ballast weights in position and take final measurements for the mass and inertia properties.

5.8 FEM Correlation

Correlation of the finite element model (FEM) with the actual physical hardware is usually an important step in the flutter model design process. In an ideal case the FEM will represent the scaled design characteristics of the "real" aircraft, and the model hardware is tuned and ballasted to match. In most cases it is impossible to achieve a perfect correlation in this manner because of certain design tradeoffs that must be made to accommodate mounting the model, instrumentation requirements, safety factors, and practical limitations imposed by material properties and fabrication processes. The approach that is normally taken is to match the model hardware theoretical FEM as closely as is practical, and then to modify the FEM to match the hardware. This modified FEM is normally a second analytical model which is then directly compared to and validated by the wind tunnel test data. Additional modifications to this FEM may be made based on the wind tunnel test results.

Generally the FEM correlation process consists of matching the FEM of each individual component against the measured (calibrated) data from that component in isolation. Then the overall FEM is correlated to the overall assembled model calibration results.

6.0 LOAD TESTS TO VERIFY STRUCTURAL INTEGRITY

The design constraints imposed by having to meet scaled mass and stiffness distributions typically will not allow flutter models to meet strength requirements with large factors of safety. Some methods of construction used on flutter models also make it difficult to accurately predict stress levels – particularly since many of the components are relatively flexible compared to force models. For these reasons it is very common for load testing to be part of the "buyoff" criteria by which flutter model hardware is accepted.

6.1 Point Loads

Point loads are often used when the flutter model construction includes internal spars or structure which carry the majority of the loads. Loads applied at the appropriate locations can be used to verify the structural integrity of the spars, flexures, and bolted attachments. In cases where a point load must be applied to a composite structure, a metal or wood block may be temporarily bonded to the composite structure to act as an attachment point.

Weight pans and Spring scales

The most common method for applying point loads to flutter model components is through the use of weight pans. Weight pans can be attached with bolts, suspended from cables, or hung from a simple "S" hook as shown in **Figure 6.1.a**. Occasionally, calibrated spring scales similar to those used by fishermen are used.

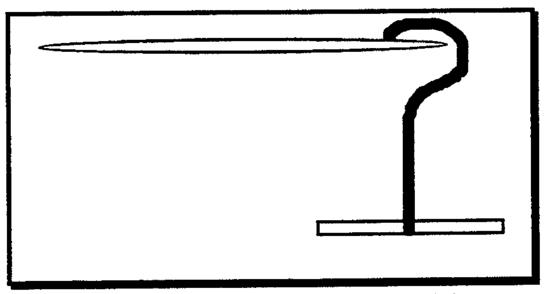

Figure 6.1a Typical Weight Plan

Hydraulic Actuators

In cases where the point loads to be applied are extremely high a hydraulic actuator can be used. Attachment to the structure is usually done by bolting directly to a spar or a metal hardpoint mounted in a composite structure. A load cell positioned between the hydraulic actuator and the model component can be used to measure the applied force. **Figures 6.1.b** and **6.1.c** illustrate some typical test setups.

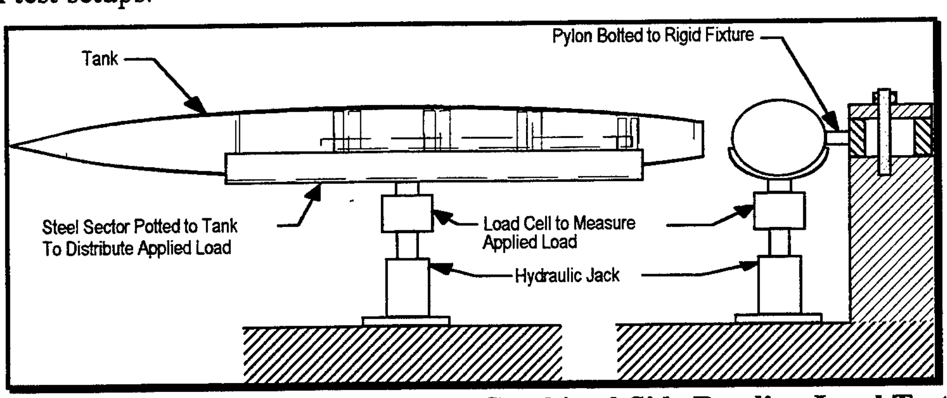

Figure 6.1b External Fuel Tank and Pylon Combined Side Bending Load Test Setup

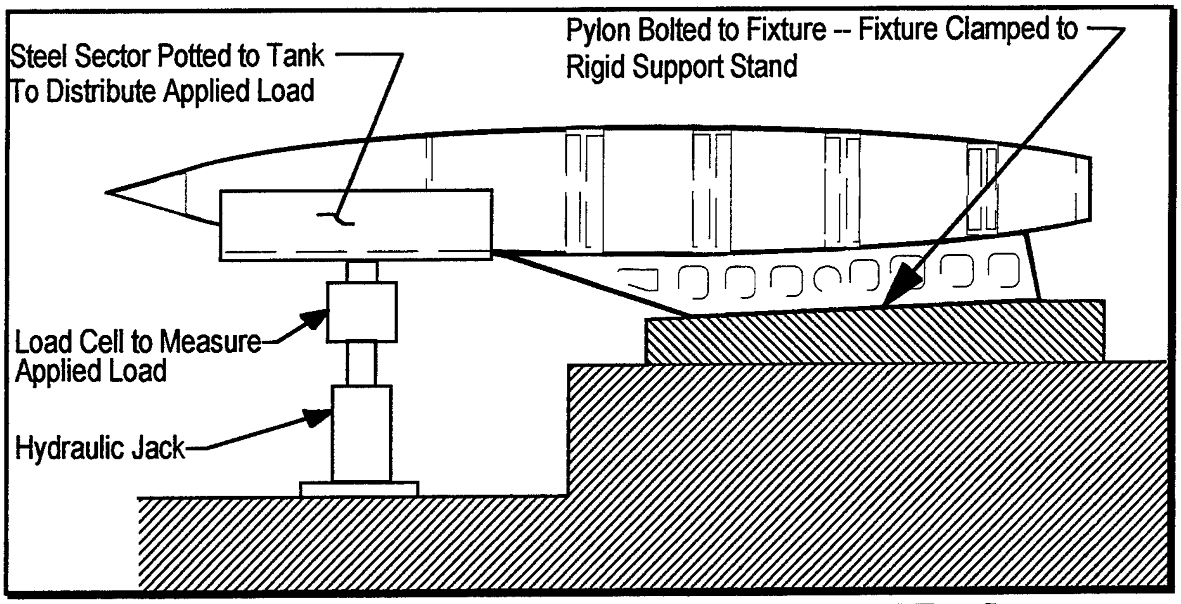

Figure 6.1c External Fuel Tank and Pylon Vertical Load Test Setup

6.2 Distributed Loads

Distributed loads can be applied to stressed-skin components or to the external panels mounted on internal spar structure. For some stressed-skin components it is necessary to apply distributed loads because loading at discrete points could damage the structure locally. For this reason distributed loads involve bags or bladders which will conform to the local contour of the surface to which the load is being applied.

Sandbags or Bags of Lead Shot

Bags filled with sand or lead shot provide a simple method for applying a distributed load to the surface of a flutter model component. Bags of a known weight can be added as necessary to achieve the required distribution. One advantage of this approach is that the distribution can be varied in different areas by stacking up different heights of bags. A disadvantage of this approach is that a considerable amount of weight may be involved, and if a failure should initiate, it will tend to progress catastrophically because the load is not self-relieving.

Water Bladders

Water bladders have an advantage over sand or lead shot bags in that it is possible to arrange the test so that the load is self-relieving. However, the disadvantage to using a sing water bladder is that only a constant pressure distribution can be applied.

Water bladders were used successfully to apply distributed loads to the supersonic wing, vertical, and horizontal components described in Section 8.0. The following description is for the particular setup used on the wing.

The purpose for performing the load test on the first production flutter model wing was to validate the handbook stress calculations and FEM stress analysis results for the wing design and to ensure that no critical failure modes were missed. A latex bladder filled with water was used to apply an even pressure distribution across the surface of the wing for the load test.

A fixture attached to the root end of the lower wing mold was used to mount the wing so that it was cantilevered 3/8" above the mold surface. The aileron was not installed on the sample. A bladder slightly larger than wing planform was formed by folding over a .030" thick latex rubber sheet and sealing the edges with vacuum bag tape. This flexible rubber bladder was placed in the 3/8" gap between the mold surface and the lower surface of the wing sample. A .008" thick piece of dry fiberglass fabric was placed between the bladder and the wing surface.

A series of wood blocks (2" x 2" cross-section) were positioned around the wing planform approximately .05" to .1" ahead of the LE, outboard of the tip, and behind the TE. These blocks were placed on top of the edges of the bladder and the fiberglass fabric, and clamped down to the mold. The fiberglass fabric was left quite loose to allow the rubber bladder to expand to completely fill the cavity formed by the mold surface on the bottom, the lower wing surface on the top, and the wooden blocks on the sides. This is illustrated in **Figure 6.2**.

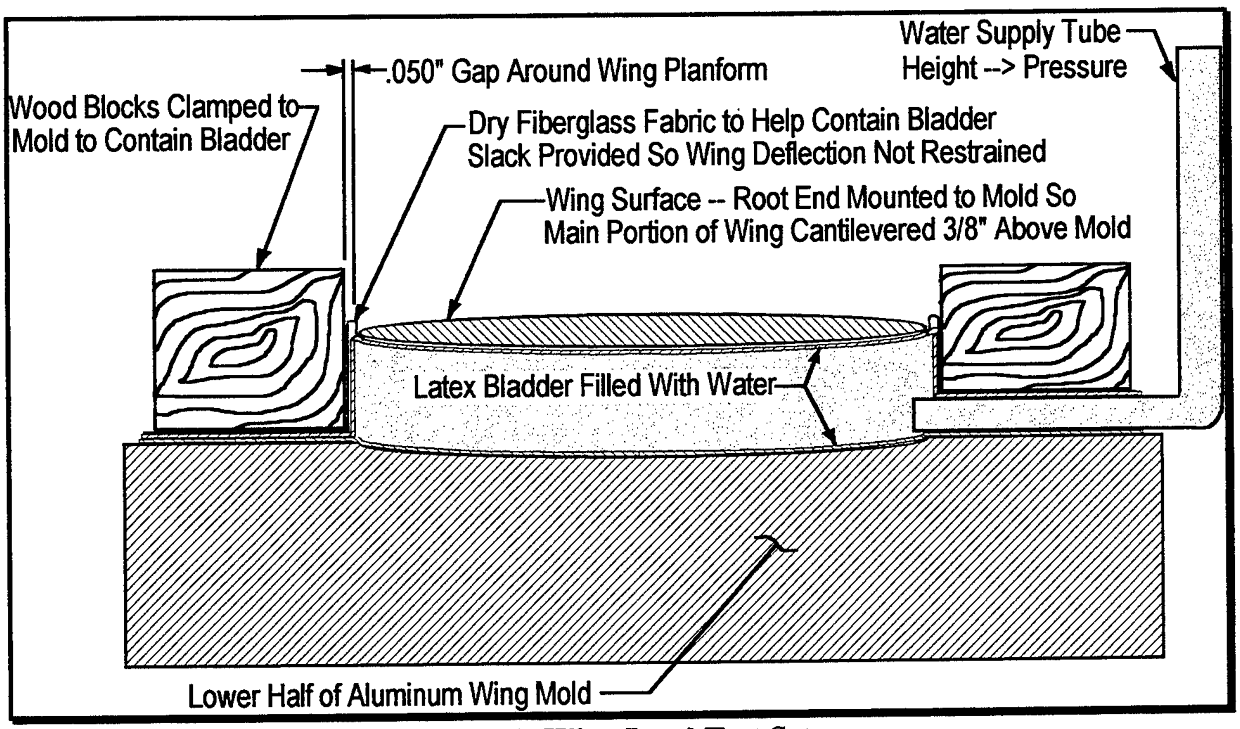

Figure 6.2 Wing Load Test Setup

In the area of the aileron cut-out an aluminum plate with a fitting for tubing was used instead of a wooden block. Clear plastic 3/4" ID tubing was attached to this fitting and marked at one intervals along its length. This tubing extended straight up from the fixture to a height of 20 feet. Blue dye was added to water to make the level in the tube more visible. A video camera was used to document the load test procedure.

Water was poured into the clear plastic tube by a technician standing approximately 16 feet above the wing. The water was poured in small amounts and the resulting water level in the tube was noted. Initially there were occasional bubbles which traveled up the tube (from the small amount of remaining air trapped in the bladder).

The tip of the wing deflected upward with each increment of water added. A scale with inch markings mounted near the wing tip was used to check the surface deflection under load. The final wing design was tested to an applied load of four psi across the entire wing surface. Deflection at the maximum load was approximately 2.6 inches. After the wing was removed from the load fixture a visual examination and frequency checks confirmed that there was no damage or change in the dynamic characteristics of the wing.

One of the distinct advantages of using a water bladder as previously described is that the load is immediately reduced once failure occurs. In a test of a horizontal component taken to failure the compression surface of the composite structure buckled due to the core honeycomb failing in compression/shear. As soon as the failure began to occur the deflection of the surface increased a fraction of an inch. This small additional displacement of the surface equated to a relatively large volume increase in the latex bladder. The water from the vertical tube immediately entered the bladder and the pressure immediately dropped. This occurred quickly enough so that further progress of the component failure was halted. This made it very easy to identify the specific mode and location where the failure initiated.

7.0 DOCUMENTATION

Documentation normally associated with a flutter model consists of a calibration report documenting all the measured properties of the model, a stress analysis report showing that the model meets all the safety criteria required by the test facility, and occasionally a stability analysis for the model installed on the particular support system to be used in the tunnel.

7.1 Calibration Report

The calibration report typically includes the measured mass and stiffness properties, the measured frequencies and mode shapes, and the documentation of any correlation work done to match the FEM to the measured data.

7.2 Stress Report

The stress analysis report typically consists of basic handbook calculations verifying the structural integrity of joints, fasteners, etc. as required by the particular wind tunnel test facility. For some models (particularly stressed skin or replica construction) the stress analysis may include stress distributions generated by a FEM.

The stress analysis report normally will also include the results from any load testing done on model components or assemblies.

7.3 Support System Stability Analysis

Frequently the support system/model assembly configuration will require a stability analysis to verify a safe operating envelope for the planned test conditions. Sometimes this analysis is done by the test facility, and sometimes it is done by the model design group. There are generally specific guidelines for a particular facility, and in some cases a custom analysis software package exists. If a support system stability analysis is done by the model design group then the results should be included in the documentation package for the model.

8.0 THE DESIGN AND ANALYSIS PROCESS – A CASE STUDY

This section describes the design and analysis process for portions of a supersonic flutter model developed by the author. This model program required stressed-skin construction for F-22 wings, horizontal tails, and vertical fins. These surfaces were tested as individual components cantilever mounted with root fairings to the wall of a blow-down wind tunnel facility. Due to large tunnel startup/shutdown shock loads and relatively high flutter frequencies, it was anticipated that only one or two flutter data points would be obtained from a component before it was damaged. Therefore, multiple test articles for each surface were fabricated and "tuned" to match a target set of dynamic specifications. **Figure 2.2*a*** of this paper documents the set of wings which were produced under this model program. The following figure shows one of these wings under construction.

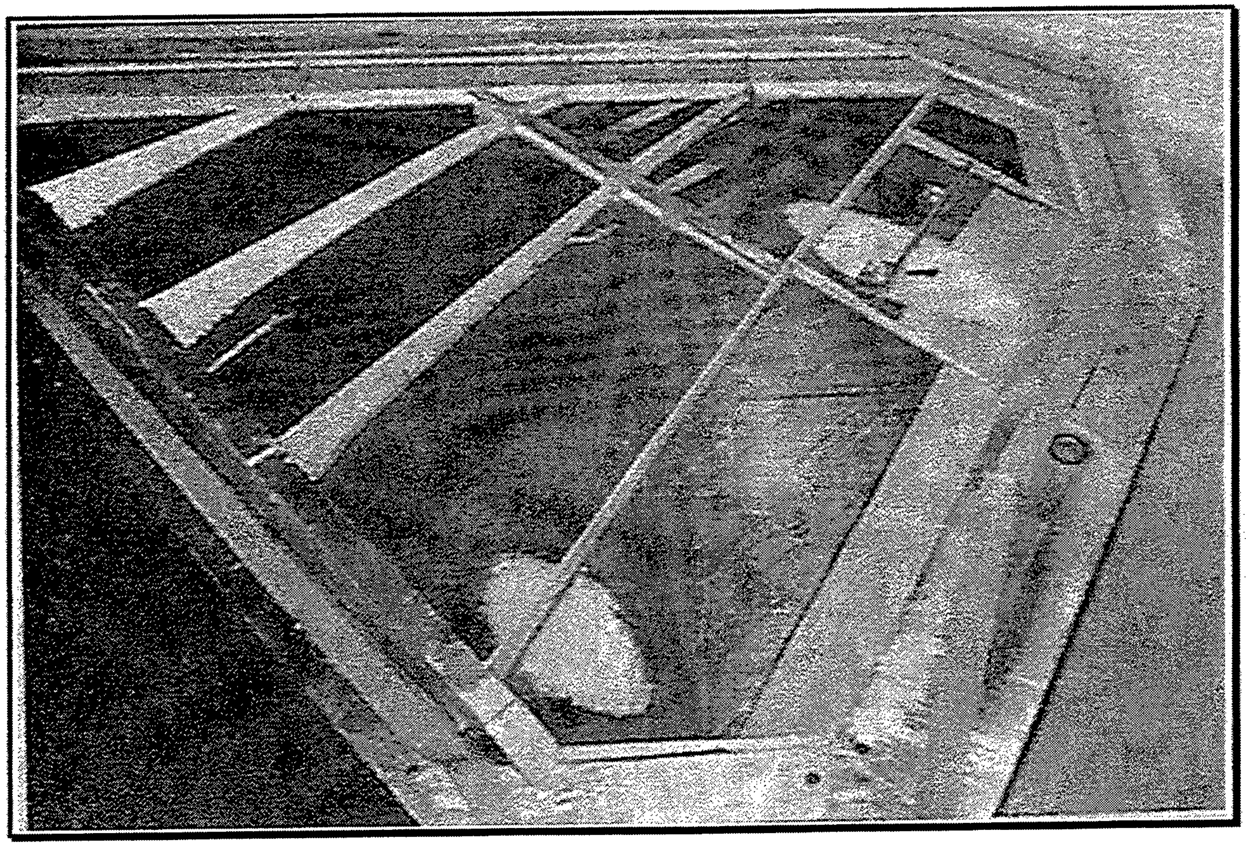

Figure 8.0 F-22 Supersonic Flutter Model Wing Under Construction

Since the design of spar elements has already been covered extensively in Section 3.2, the following subsections will concentrate on the design and analysis process for stressed-skin construction with an emphasis on one particular surface (the vertical stabilizer) and its associated design considerations.

8.1 Methodology For Converting Specifications

For each surface the simplified full scale layup for each segment of each skin was analyzed using a composite laminate analysis program to determine equivalent stiffnesses for the full layup in each direction. This stiffness was scaled by the desired scale factor and, using a PC spreadsheet routine, converted into a table of equivalent stiffnesses and corresponding skin thicknesses. (Model-scale skin thickness was not necessarily equal to the linear scale factor times full-scale thickness.) Based on the materials selected for the basic skin layups (reference Section 8.2) proposed layups were developed and analyzed using the same laminate analysis software to match the equivalent skin stiffnesses in all directions as closely as possible.

After a skin layup was determined, the data for this layup and possible structure was input into weight and stress analysis spreadsheets which were developed for each surface. An overall evalaution of strength, mass properties, and stiffness sometimes resulted in conflicting requirements (i.e., to achieve the required stiffness might result in a mass distribution which did not match the target specification). When this occurred, the results and possible alternatives were discussed and analyzed. Modifications to the target specifications were necessary for all three surfaces, but these modifications were made in a way that preserved both the general characteristics of the flutter mechanism, and the proper relationship between critical modes.

The final model design specifications were then converted to the fabrication drawings and process control sheets used to produce the final hardware.

8.2 Material Selection and Property Verification

The model specification conversion process generated target layup stiffness, strength, and mass property requirements. To satisfy these requirements a prepreg unidirectional graphite was chosen as the primary skin layup constituent because of graphite's high stiffness-to-weight and strength-to-weight ratios. The thinnest readily available material (.003" thick) was chosen to allow the greatest flexibility in developing specific layups to match targets. Continuous fabric was used on the outer layer of each layup to reduce the risk of bumps or scrapes causing local delaminations. Fiberglass was chosen because it was available in the thinnest stock (.0015" thick).

Paper honeycomb core material was chosen because of its high strength-to-density ratio. The specific density used in each surface was determined based on a stress analysis of the composite surface at critical sections. Honeycomb in densities of 1.8, 3.0, and 6.0 pounds/cubic foot was used in the various surfaces.

After the initial selection of materials various sample coupons were used to verify the stiffness, density, and strength characteristics of each. A shear test was done on a layup of the unidirectional graphite to confirm shear strength. Sixteen sandwich coupons were made with fiberglass/graphite skins and cores of various grades of honeycomb. **Figure 8.2** shows a typical coupon. The stiffness of these coupons was tested using the mirror calibration

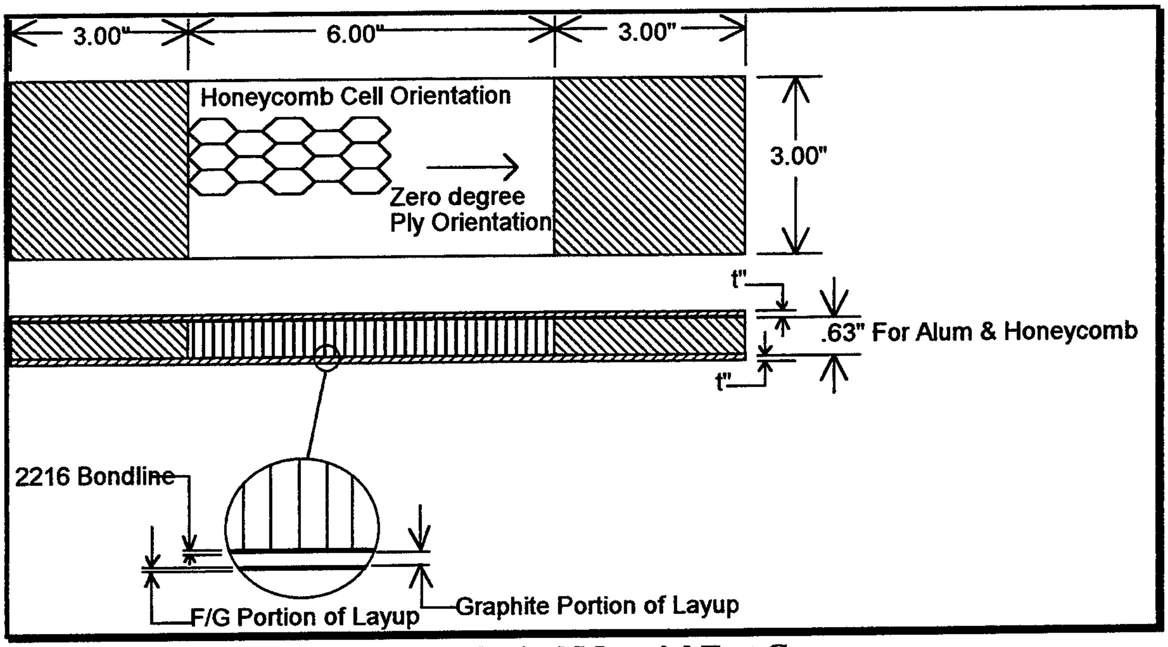

Figure 8.2 Typical Material Test Coupon

8.3 Stiffness and Strength Evaluation

The stiffness of the horizontal tailboom spar was tested using the mirror calibration technique, and also by measuring deflections with dial indicator gages (accurate to .0005") as loads were applied. The stiffness of the production composite components was not directly measured. Determination of mass properties, frequencies, and node line positions was used to indirectly verify the stiffness of each component.

Mirror calibration was used to evaluate the horizontal actuator flexure stiffness when mounted in the tailboom. All other flexure stiffnesses were evaluated indirectly and modified based on frequency and mass property data. This was more consistent with the fact that the specified data were loop spring rates (they included the backup stiffness of the structure which the flexure was mounted to).

The strength of built up structures was initially evaluated by a stress analysis. Because of the extreme loading conditions anticipated for the test, proof load testing was also done on each surface and store. For the vertical fin, horizontal, and wing the surface was cantilevered at the root as it would be installed in the tunnel, and an even pressure was applied to the entire planform area using a water-filled latex bladder as described in Section 6.2. For the external stores a hydraulic jack/load cell combination was used to apply loads as described in Section 6.1.

8.4 Weight Evaluation and Control

Weight evaluation and control included the development of realistic weight targets during the design phase, control of weight during the fabrication phase, and verification for the final as-built surface.

Densities for materials commonly used for flutter model construction have been evaluated and tabulated during previous flutter model programs. For materials specific to this program, such as the prepreg unidirectional graphite and the fiberglass fabric wet layup, sample coupons were fabricated using the same processes anticipated for the actual hardware. The densities derived from these samples and from previously tabulated information were used to develop a weights spreadsheet for each component surface. The spreadsheet divided the surface into the individual weight cells defined by the surface FEM. For each cell the volume and density of individual items were separately tabulated. A typical weight cell would include data for some or all of the following:

- Upper skin layup
- Lower skin layup
- Honeycomb core
- Plywood rib or spar segments
- Aluminum or steel hardpoints
- Instrumentation & wiring
- Adhesive (glue)
- Ballast weights

The spreadsheet allowed weight, CG, and inertia evaluations for individual components of a cell, cell totals, or combined values for the entire surface.

During fabrication the amount of resin to be used for each layup was specified in the written fabrication process. The amount of adhesive was also tightly controlled. The labels on **Figure 8.4** indicate all the individual components of the internal wing structure. A two-page table recording the target and actual amount of glue applied to each of the indicated components was included in the fabrication process for each wing.

Some of the initial sample surfaces were cut up into segments corresponding to the weight cells defined in the spreadsheets and the FEMs. The weight of individual segments was compared against predicted targets and, if necessary, adjustments were made to the targets and the written process sheets prior to fabrication of the production parts.

The mass properties (weight, CG, and inertias) for each production surface were measured and compared to the predicted values. For the wings a final adjustment was made by adding a small amount of ballast to each of the wings in the aileron cove area. The amount of ballast was chosen to produce the best matched set of final production wings.

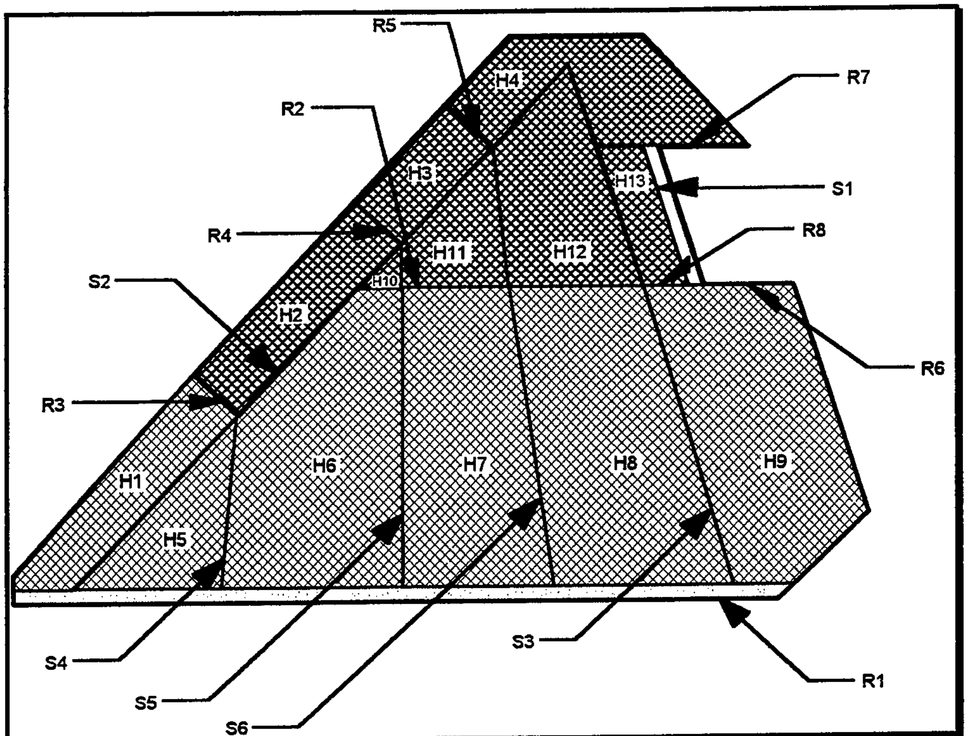

Figure 8.4 Sample Figure For Glue Weight Control (Wing Fabrication Process)

8.5 Model Scale FEM

Component geometry was taken from the full scale FEM data scaled to model scale. It was modified slightly to suit tunnel connection requirements. Internal geometry was simplified as much as possible without violating structural integrity or mode shapes.

The flutter model components were fabricated from fiberglass and graphite composite materials, paper honeycomb, balsa wood, plywood, steel, and aluminum. The composite materials and the paper honeycomb were orthotropic materials. The moduli of elasticity for all these materials were measured and the nominal values were included in the finite element models.

FEM Generation and Ground Rules

The purpose of the FEMs was twofold: first, to aid in the design of the flutter model so that the mass properties, stiffness distribution, natural frequencies, and mode shapes reasonably represented the full scale design, and second, to provide a high quality analytical model that closely matched the fabricated flutter model.

Mass distribution data was provided (in full scale) for all the components as a series of lumped masses. Data representing the stiffness distribution, frequencies, and mode shapes of the full scale aircraft were dynamically scaled, and the resulting mass and stiffness distributions were used as a guide to design the flutter model components.

Components were designed to match as closely as possible the scaled mass and stiffness distributions of the full scale aircraft. Operationally, this meant matching the first five mode shapes and frequencies to within 5% of the measured values.

FEM Tuning

Samples of each component (wing, horizontal, and vertical) were built. These samples were weighed and the mass properties (CG and inertias) were measured. Some samples were carefully cut along prescribed lines so that a detailed comparison of the mass distributions could be made. Results of the mass measurements were used to modify the mass distributions of the component FEMs to reflect more closely the fabricated parts. No structural influence coefficient measurements were made for any supersonic flutter model component. Overall stiffness was measured indirectly by matching mode shapes and natural frequencies.

The sample wing was experimentally tested to determine its natural frequencies and mode shapes in both the supported and unsupported configurations, with and without the aileron. The aileron itself was also tested to obtain unsupported frequencies, and again supported on flexures that were fixed to ground. All this data was used to modify the wing and aileron FEM to match more closely the fabricated parts.

The sample horizontal tail was also experimentally tested in both the supported and unsupported configurations. The horizontal tail was initially tested independently of the tailboom. The experimental data was used to tune the horizontal FEM, and more tuning was done later when the tailboom became available for testing. The tailboom was examined by itself, then with the horizontal attached to it. This information was used primarily to design and model the horizontal pitch spring.

The vertical tail sample components, fin and rudder, were tested individually and combined. The fin was tested by itself in both the supported and unsupported configurations. The rudder was tested unsupported, and then supported on the hinges that were fixed to ground. Then the fin and rudder combination was tested in both the supported and unsupported configurations. This data was used to tune the fin, rudder, actuator spring, and hinges of the vertical FEM.

8.6 Model Stress Analysis

The purpose of the stress analysis was to verify the structural integrity of the flutter model component designs so that they could perform their missions safely. Each surface was checked for tensile strength, compressive buckling, and core shear. Hinges, flexures, and screw fasteners were checked for load carrying capacity.

Satisfactory strength was an important part of the design criteria. It was necessary to insure that each component of the flutter model could withstand the wind tunnel starting shocks. No data could be obtained if the structure failed before achieving a flutter condition. Each component of the flutter model was designed to have a safety factor of 1.5 based on ultimate stress.

Applied loads were estimated initially from data provided in text books. The design pressure was specified as 4.0 psi based on actual wind tunnel measurements. The skin of each surface could survive 8.8 psi with more than 1.5 factors of safety based on tensile strength, but subsequent tests showed that the failure mode was core buckling, not tensile strength. The designs were changed to incorporate a stronger (though heavier) core that could survive a 4.0 psi starting load.

Easy to apply, basic handbook equations were used to estimate the strength of the component designs. Many equations could be found in standard texts on stress analysis. Some of the formulas, especially those pertaining to core buckling, came from the HEXCEL design manual. Later, when representative finite element models were generated, detailed stress distributions were computed for verification of the hand analyses.

Cross sections for critical stress areas were evaluated for each component. Section properties for complicated geometries were computed using the CAD system. A FORTRAN program was written that computed orthotropic properties for composite material lay-ups. Applied forces and moments were conservatively derived and used in the calculation of stress.

Material properties were obtained from a variety of sources including in-house testing. Material properties for standard structural materials like steel and aluminum were obtained from MIL HANDBOOK 5. For composite materials like fiberglass and graphite, some, but not all, material properties could be found in vendor (FIBERITE) catalogs. Data for the paper honeycomb core came from the HEXEL catalog. Other properties for composite materials, and for balsa and plywood, were obtained by performing calibration tests.

After the designs were approved, sample components were built. These samples underwent a variety of tests for mass properties, vibration characteristics, and strength. Eventually, the samples were tested to failure to measure their load carrying capability, and to ensure that all failure modes were accounted for.

8.7 Vertical Stabilizer Construction Details

As shown in **Figure 8.7a** the vertical stabilizers were fabricated as individual fin and rudder components which were then assembled with flexure springs and a hingeline skirt.

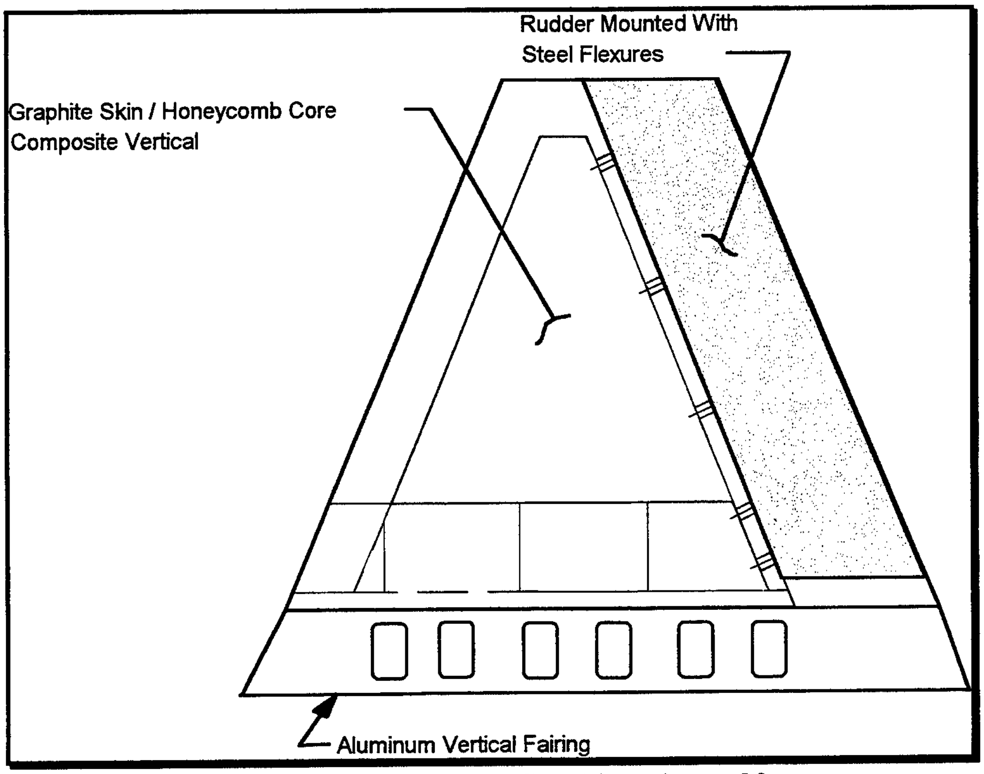

Figure 8.7a Vertical Stabilizer Assembly

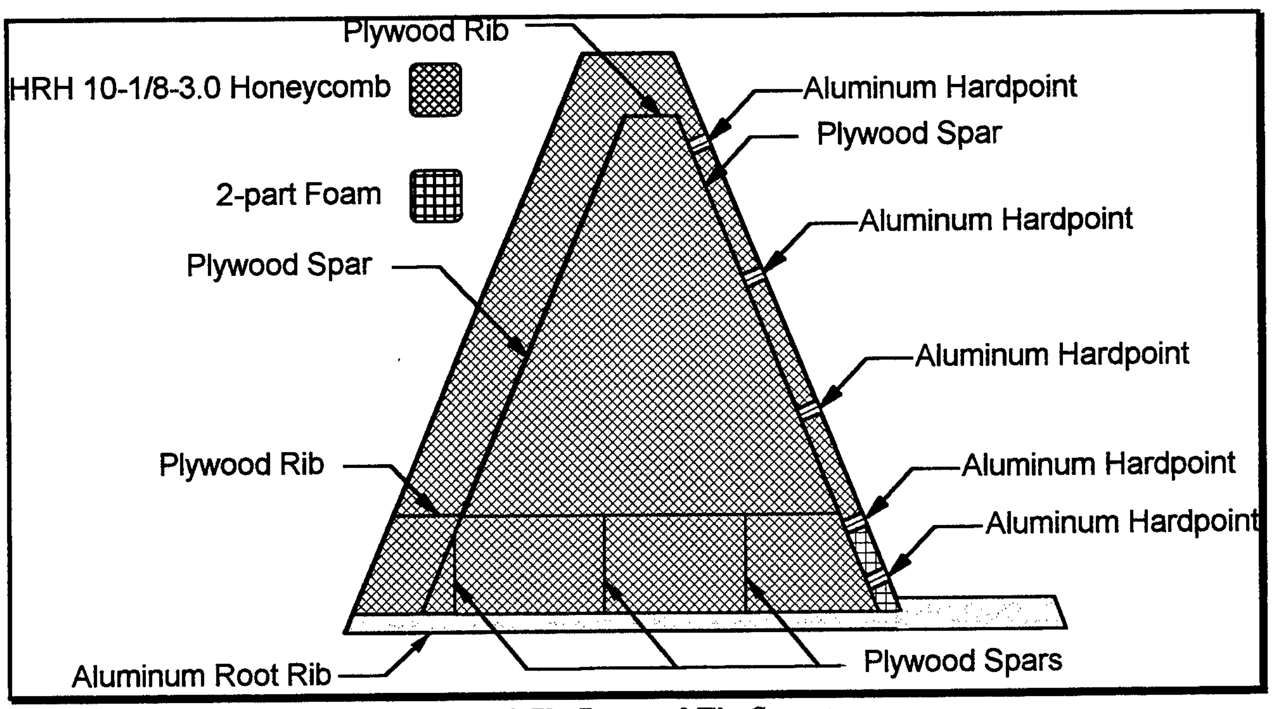

Figure 8.7b Internal Fin Structure

Fin Construction

Figure 8.7b shows the basic internal structure of the vertical fin. The aluminum root rib had 1/4-20 keenserts and dowel holes installed to mount to the vertical fairing. In the hingeline area the rib had a pocket machined out to provide a mating surface for the rudder actuator flexure. Five aluminum rudder hinge hardpoints were bonded to the inside of one skin with additional plywood support structure. All other spar and stiffeners were 1/16 inch thick aircraft plywood. The location of the internal structural components was matched to the full scale aircraft wherever possible to maintain similar load transference paths and mass distributions. The paper honeycomb core density was three pounds per cubic foot.

Fin skins had fiberglass fabric outer layers and internal graphite unidirectional plys at specific orientations to match the desired stiffness and mass distributions. The layups for the upper and lower skins for the fin were not identical, but reflected the asymmetry of the full-scale aircraft vertical fin. Instrumentation included one accelerometer and two strain gage bridges.

Rudder Construction

The upper and lower rudder fiberglass and graphite skin layups were asymmetric, corresponding to that used on the full scale aircraft. Internal structure consisted primarily of balsa and plywood stiffeners. At each of the five rudder hinge locations an aluminum hardpoint was bonded to the skin, and a sixth larger aluminum hardpoint was bonded in to provide attachment for the rudder actuator flexure. The paper honeycomb core material had a density of 1.8 pounds per cubic foot. One accelerometer was installed in the rudder.

Mounting Hardware

The rudder is mounted to the vertical by X-flexures at five hinge point locations. Construction of the X-flexures is shown in **Figure 8.7c**. Two wire EDM stainless steel flexure webs are assembled with aluminum spacer blocks to create a flexure assembly. Each end of the X-flexure is mounted to a hardpoint in the vertical or rudder with two #4-40 flat head cap screws.

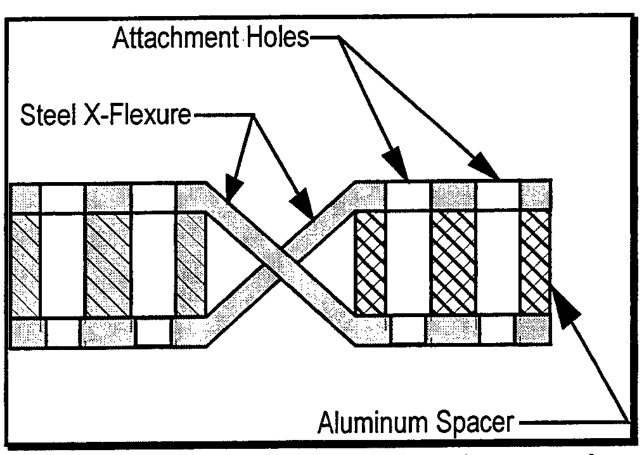

Figure 8.7c Rudder X-Flexure Construction

X-flexures were chosen to eliminate concerns about the friction and damping which would be present with pin or bearing attachments. The X-flexures provided a very low hingeline springrate, and a separate torsional flexure was used to model the rudder actuator stiffness. The outboard end of the rudder actuator flexure was attached to the rudder through a friction ring clamp with two set screws providing positive mechanical location. The root end of the actuator flexure was rigidly bolted to an extension of the aluminum root rib for the vertical.

The root rib of the vertical was attached to an aluminum vertical fairing assembly with twelve 1/4-20 socket head cap screws and two dowel pins. The vertical fairing assembly was in turn mounted to the interior window plate with ten 1/2-13 socket head cap screws. This vertical fairing assembly continued the external vertical contour inboard to the fuselage intersection plane. The fairing was machined from a single block of aluminum with six pockets on each surface to provide access to attachment bolts.

Hingeline Skirts

The magnitude of the start-up shocks and the size of the rudder resulted in a requirement for large bending moment loads to be transmitted across the rudder hingeline. Stress calculations indicated that the load would need to be distributed along the entire hingeline. Transference at a select number of points would locally overstress the skins of both the vertical and the rudder. A single layer of Kevlar fabric was bonded across the hingeline gap along the entire span of the rudder. This Kevlar "skirt" was impregnated with RTV resin in the gap area to allow it to remain flexible and not dampen the motion of the rudder surface within a $\pm 3.5°$ of deflection.

At approximately 3.5° the skirt on one surface would become taunt and transmit tensile loads between the rudder and the vertical. Along the opposing surface the gap closed so that the skins of the vertical and rudder made contact and transmitted compressive loads. A thin rubber strip bonded to the vertical side of the gap helped ensure that the compressive loads were more evenly distributed along the length of the hingeline. **Figure 8.7d** shows the hingeline area with the rudder in nominal position during testing and also at a rudder deflection of 3.5°. The bending moment produced by the start-up shock impinging on the rudder was taken out through tension in the skirt and compression through the skins. The shear loads were carried by the X-flexures located at the hinge points.

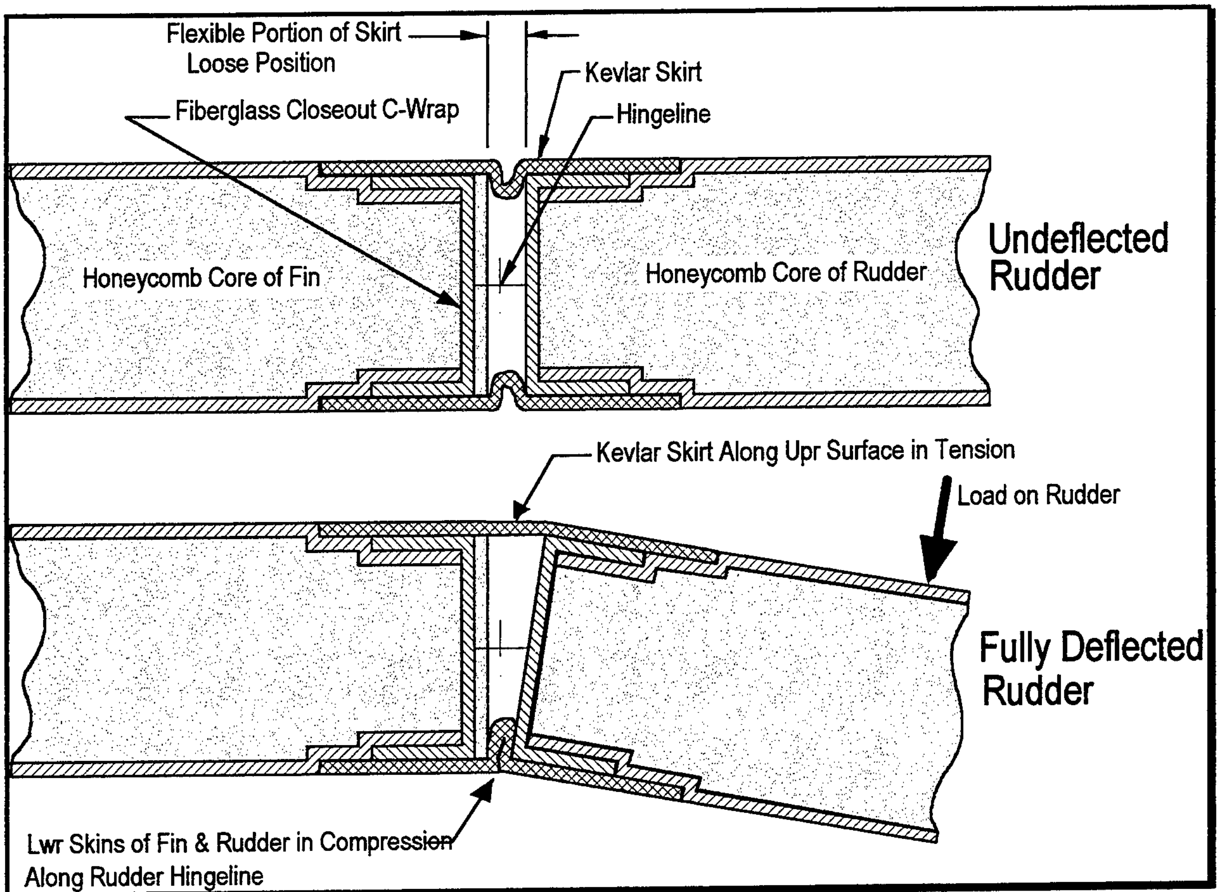

Figure 8.7d Rudder Hingeline Skirt Construction and Load Transference

Rudder Actuator Stiffness

The nominal rudder flexure configuration is shown in **Figure 8.7e**. The flexure is primarily a torsion flexure, although there is a small component of bending due to flexure centerline being offset from the hingeline. The square portion of the part acted as the actual flexure. The length of this square portion was extended to produce reduced stiffness flexure configurations. A 50% rudder flexure therefore has a two inch flexure length (twice the nominal).

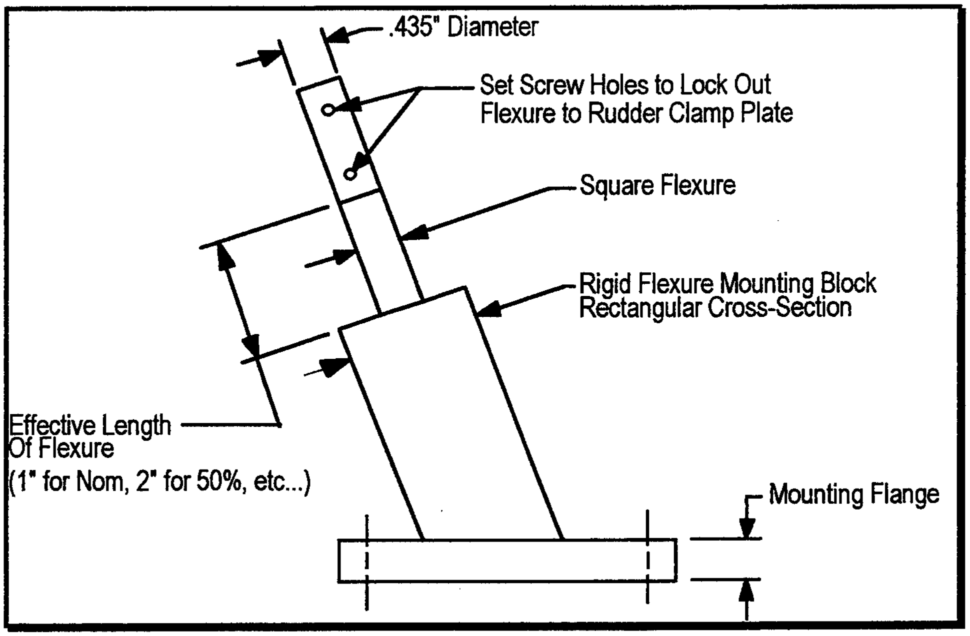

Figure 8.7e Rudder Actuator Flexure

Vertical Ballast Cases

To test a second ballast condition for the vertical, lead foil tape (.006 inches thick) was added to the exterior skin on the upper and lower surfaces of the vertical and rudders in the areas indicated in **Figure 8.7f**.

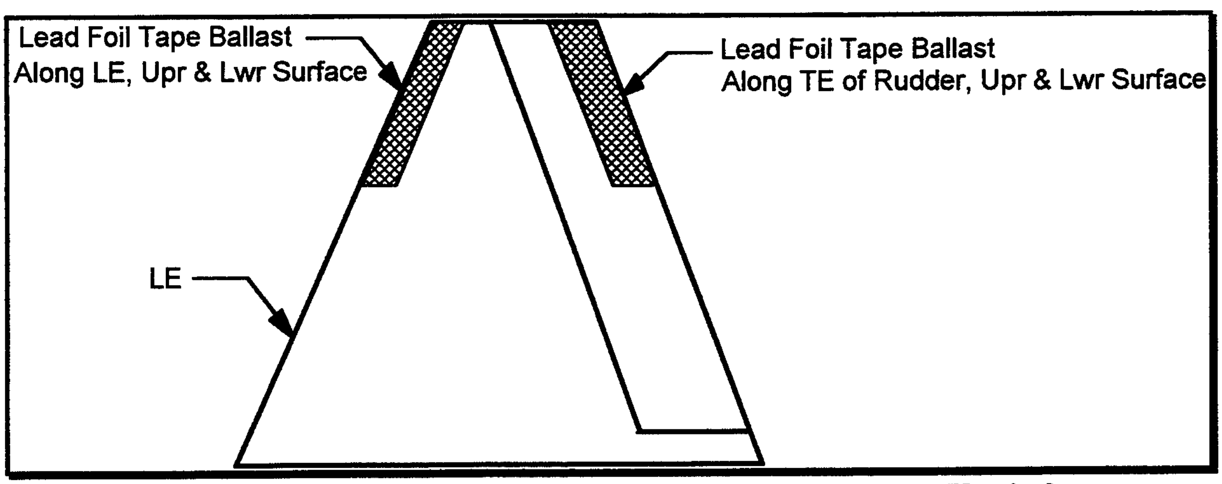

Figure 8.7f Location of Additional Ballast Added to the Verticals

Conclusion of Case Study

The F-22 supersonic flutter model components described in this case study were successfully tested at the Rye Canyon blow-down facility in Valencia California in 1994.